5-2017

Total synthesis of barettin: Model study of specialized aldol condensation to directly access diketopiperazine targets

Elizabeth W. Kelley
College of William and Mary

Total synthesis of barettin: Model study of specialized aldol condensation to directly access diketopiperazine targets

A thesis submitted in partial fulfillment of the requirement
for the degree of Bachelor of Science in the Chemistry Department from
The College of William and Mary

by

Elizabeth Wells Kelley

Accepted for __Honors_____
(Honors or no Honors)

_____
Jonathan Scheerer, Chemistry, advisor

_____
Elizabeth Harbron, Chemistry

_____
Robert Hinkle, Chemistry

_____
Jonathan Allen, Biology

Williamsburg, VA
May 2, 2017

Table of Contents

Introduction.....2

Antibiofouling: a rock and a hard place.....2

Barettin, the target.....3

Diketopiperazines and the aldol condensation: access to privileged bioactive scaffolds.....5

Results and Discussion.....8

*The first aldol condensation: degradation of **9** and **10***.....10

*The second aldol condensation: rearrangement of **12** into **15***.....12

*Boc-acylation of **12**: a separation issue*.....13

Conclusion.....13

Future Directions.....13

Contact Information.....14

Abbreviations.....14

Experimental.....14

Acknowledgements.....17

References.....18

Supporting Information.....20

Introduction.

Antibiofouling: a rock and a hard place.

Biofouling, the attachment of organisms to wet surfaces such as ship hulls, pipelines, power stations, and oil rigs, costs the global economy an estimated $1 billion per year directly[1] and presents several environmental and human health consequences. Underwater surfaces accumulate up to 150 kg of biofouling mass per square meter[2], and some biofouling organisms employ boring and adhesion techniques which cause physical damage and could threaten the structural integrity and functioning of submerged infrastructure.[3,4] The increased drag and weight on ship hulls can lead to 40-50% increased fuel consumption[2,4], causing an additional estimated 7.3 million tons of fuel consumed and 23 million tons of CO_2 and 750,000 tons of SO_2 burned per year[5] as well as significant increases in time and money spent in maintenance, wasted resources, and lost shipping time.[2,4,5] As a result, voyage costs can increase by 77%.[5] On stationary infrastructure, biofouling causes structural integrity concerns due to surface deterioration and additional weight. Non-indigenous species also piggyback on ocean liners and threaten the biodiversity and stability of distant ecosystems[2,4]; an estimate of the economic damage done within the United States by non-indigenous species was recently calculated as $137 billion per year.[6] The antibiofouling market was valued at $4 billion in 2009[7], and the marine coatings market alone was valued at $7.67 billion in 2013 with a projection to rise to $11.88 billion by 2020.[8] The economic and environmental consequences of biofouling are therefore serious international issues.

Pictures 1-3. Examples of biofouling and boring.[9]



Maritime civilizations throughout the ages have employed antibiofouling methods to combat these problems, from attaching disposable panels of wood, lead, wax, tar, etc. onto outer hulls in early Mediterranean trading vessels in the 700s BCE to copper sheathing in the 18th century British Empire to the use of biocide paints in modern times.[10] Tributyltin oxides (TBT/TBTO), which kept surfaces biofouling-free for up to 5 years, were the main active components in biocide paints used by an estimated 70% of the international shipping industries and government navies for the past 40 years.[2,4] However, the universal toxicity and bioaccumulation of organotins leeching out of the paints precipitated environmental and economic disasters, in addition to being a mammalian carcinogen[2,7], and organotins were consequently banned from biocide paints by the United Nations in 2008.[11] The global shipping industry and UN signatory governments have struggled since the ban to prevent biofouling in a market bereft of organotins, and the antifouling industry has scrambled to fill the void with less toxic alternatives. Despite the diversity of avenues being explored, there is not yet a definitive environmentally-benign and cost-effective solution to the biofouling problem which is becoming increasingly urgent.[1,4,7,10,12]

Intertanko released a statement in 2016 claiming "Since the entry into force of the [biocide paint ban], there has been no single antifouling coating which can meet all the operational conditions for a particular vessel".[13] Those currently still in use present environmental and human health concerns and may face future bans.[7,10,14] As a part of this effort, many natural marine products and synthetic derivatives have been developed and tested over the course of the past two decades for antibiofouling.[3,15] However, to the best of our knowledge, none yet meet the criteria for a successful antibiofouling agent: low toxicity, stability in a paint or on specialized surfaces, biodegradable, broad-spectrum activity, and commercially producible.[15] Barettin, a potent natural antibiofouler, may help fill this need.

Barettin, the target.

Barettin (**1**) was isolated as a secondary metabolite from the cold-water sponge *Geodia barretti* in 1986.[16] *Geodia barretti* sports a fouling-free surface, a characteristic attributed to the production of **1** which possesses potent antibiofouling activity.[17] Barettin was previously misidentified as **3**, but its structure is now definitively established as **1**.[17,18,19,20] The antibiofouling properties of **1** against barnacle and blue mussel larvae (EC_{50} = 0.9 μM = 0.4 μg/mL) cause it to inhibit settlement metamorphosis in concentrations comparable to TBT (LC_{50} = 0.09 μg/mL) in the lab and in field conditions.[17,21] Crucially, this inhibition appears to proceed in a nontoxic, reversible manner: once removed from water containing **1**, barnacle larvae continue their life cycle.[17] Barettin is proposed to be putatively nontoxic[22] and, since it is a natural product composed of amino acids, biodegradation pathways likely exist in aquatic environments. These properties could make barettin a unique antibiofouler since most antibiofoulers are active through toxic mechanisms and pose bioaccumulation risks. Besides immediate environmental concerns, toxic mechanisms apply a selective pressure for resistance development whereas a nontoxic antibiofouling agent arguably helps combat resistance: susceptible biofoulers are forced to settle elsewhere, compete with other (possibly less susceptible) species, and progenerate future generations of susceptible organisms. Barettin is also an antioxidant[22], antiinflammatent[22], selective serotonin receptor ligand[23], and AChE enzyme inhibitor[24]; its ability to behave as a selective serotonin ligand has been proposed as its mode of antibiofouling activity.[23] Neurotransmitters have been noted as one method by which planktonic larvae receive the cue to settle on a surface, so the blockage of a serotonin receptor could prevent those cues from being received. This is especially pertinent for barnacle settlement which has been shown to depend strongly on the endogenous amine serotonin[25] but also indicates that barettin may be a universal anti-biofouler agent across the animal kingdom since serotonin receptors are evolutionarily conserved.

Isolation of **1** actually produced a 87:13 Z:E isomeric mixture of **1**:**2**[17], but it should be noted that biological studies indicate only the Z isomer and not the E as the subject of their assays. No one has yet determined if there is a difference in the biological activities of the two geometric isomers or if an equilibrium exists at relevant aquatic environments. Additionally, the stereocenter of **1** and **2** was identified as *S*, but no biological differences have yet been specified from the *R* stereoisomer. There is ample room for investigating barettin to improve potency: only three barettin derivatives with modified tryptophan moieties have been tested for antibiofouling activity[26], and no literature precedents yet exist for derivatives with modified arginine moieties. Nine analogues of dipodazine have been tested, though, which suggest possible alterations to make to barettin's tryptophan side-arm.[26]

Renewed isolation efforts have revealed two additional barettin analogues, dihydrobarettin (**4**)[17] and bromobenzisoxazolone barettin (**5**)[27], both of which possess significant antibiofouling properties (EC_{50} = 7.9 μM and 15 nM, respectively). Interestingly, barettin and dihydrobarettin have been shown to exert

Figure 1. Barettin analogues and endogenous amines.

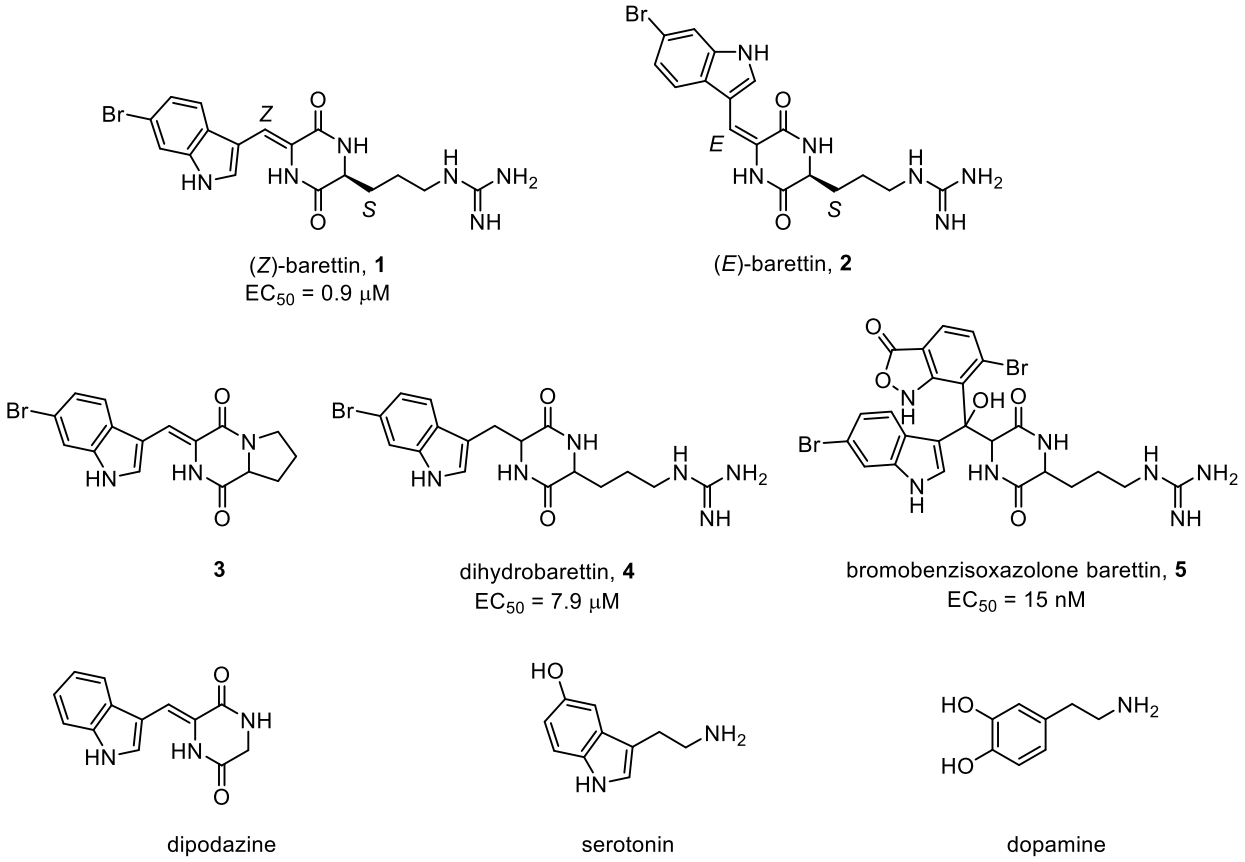

a synergistic effect against barnacle larvae.[28] It is likely, based on parallel situations and on the lack of a shikimic acid biosynthetic pathway in sponges (by which tryptophan is usually produced), that **1**, **4**, and **5** were produced by symbiotic/commensalistic microorganisms to combat settlement on the filter-feeder, saving the sponge and its microbial allies from starvation.[27,29] While **5** is 60 times more potent than barettin and also inhibits barnacle settlement in a reversible manner, **5** was isolated in less than 0.1 % yield, which likely caused it to be overlooked in earlier isolation efforts and suggests that it is not the sponge's primary mode of defense.[27] No synthetic pathway has yet been published for **5**. However, once a pathway has been devised, it will be interesting to further investigate its mode of action since it does not appear to act as a serotonin receptor ligand like barettin.[27] More studies on barettin family members are necessary to fully understand their modes of action and suitability as commercial antibiofouling agents, but they show promise.

A synthetic route to **1** via peptide coupling and cyclization (Scheme 1) was published in 2004[20], but, in the author's own words, it is "labor intensive and far too expensive for large scale production".[30] Several patents have been filed concerning barettin and derivatives for use as medical preservatives, antiinflammation, antioxidation, antirust, and antifouling agents.[31,32,33] Barettin derivatives may be suitable for several diverse future commercial applications if a commercializable route were devised. In pursuit of such a route, we targeted the diketopiperazine ring as a starting scaffold and used iterative aldol condensations to assemble the necessary functionalities (Scheme 2).

Scheme 1. Pre-existing synthetic route to barettin.

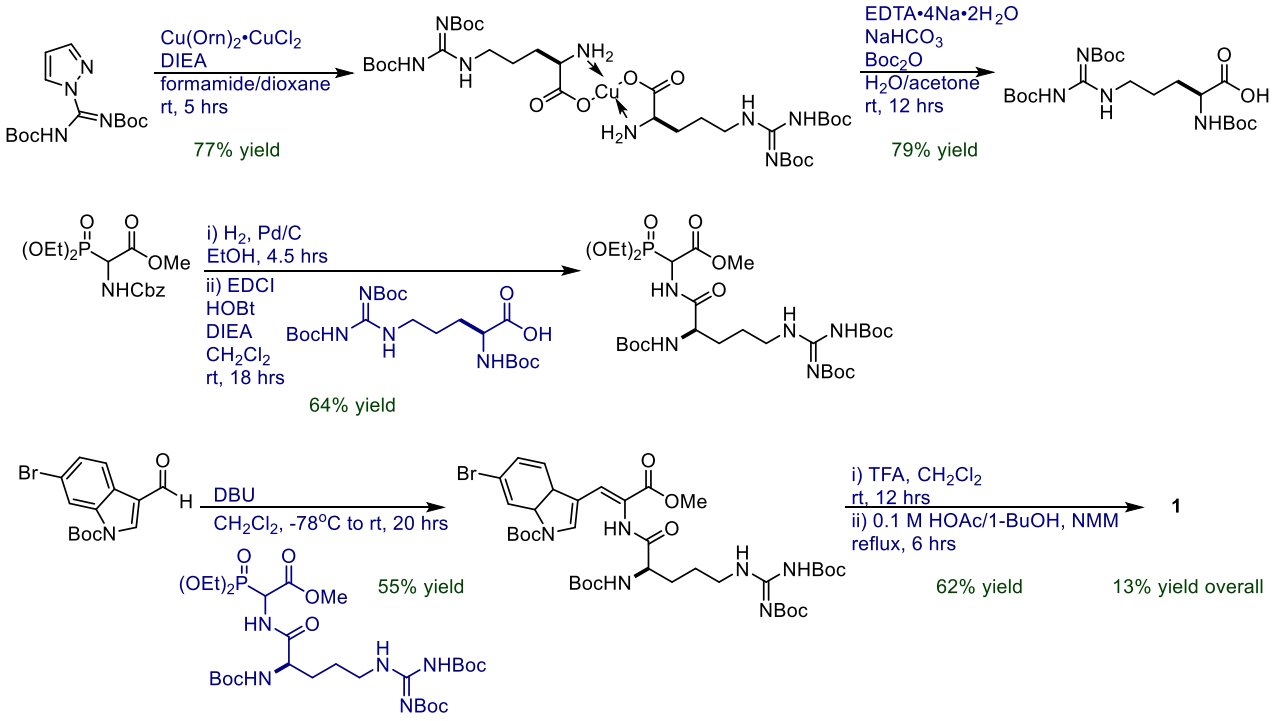

Scheme 2. Proposed retrosynthetic route to barettin using iterative aldol condensations.

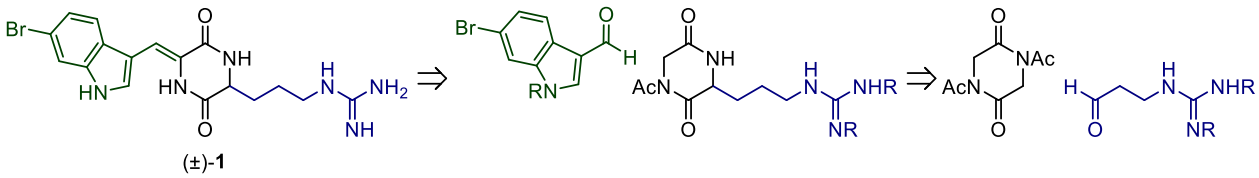

Diketopiperazines and the aldol condensation: access to privileged bioactive scaffolds.

The diketopiperazine ring (DKP, also called piperazinedione), the cyclic dimer of amino acids, is a privileged structural motif shared among numerous natural bioactive compounds and synthetic derivatives. Extensive research and comprehensive reviews over the past several decades have elucidated and compiled a host of information on the diversity of DKP structures, drug-like characteristics, natural prevalence, biological activities, potential applications, and synthetic routes. DKPs are abundant in nature and display a broad spectrum of potent bioactivities, such as antioxidation, antiinflammatory, anticancer, antiviral, antibacterial, antifungal, sexual function regulation, antihypertension, cardiovascular regulation, neuroprotection, and antibiofouling properties.[34,35,36,37,38] Many bioactive DKPs are not limited to only one bioactive property but rather possess a range of such properties. The ring's heteroatomic structure enables a variety of reactivity, and the DKP family is increasingly recognized to possess multiple favorable drug-like characteristics. The DKP ring is an inherently attractive scaffold for drug discovery due to its small size, heterocyclic structure, resistance to proteolysis, and cheap commercial availability. It is amenable to derivatization at six positions (including four proto-chiral carbons) to form chiral, non-planar, structurally diverse compounds which maintain rigid, conformationally constrained backbones. A few drugs and potential drug leads derived from this family are represented in Figure 2. Due to their amino

acid-based structures and favorable drug-like characteristics, it is likely that natural DKPs and their synthetic analogues will continue to provide interesting targets for biological study and chemical synthesis in the future. As such, the development of techniques for derivatization of DKPs is of interest to improve synthetic capabilities and enable biological investigations and scale-up commercialization of interesting DKPs.

Figure 2. A sampling of potent DKP analogues.

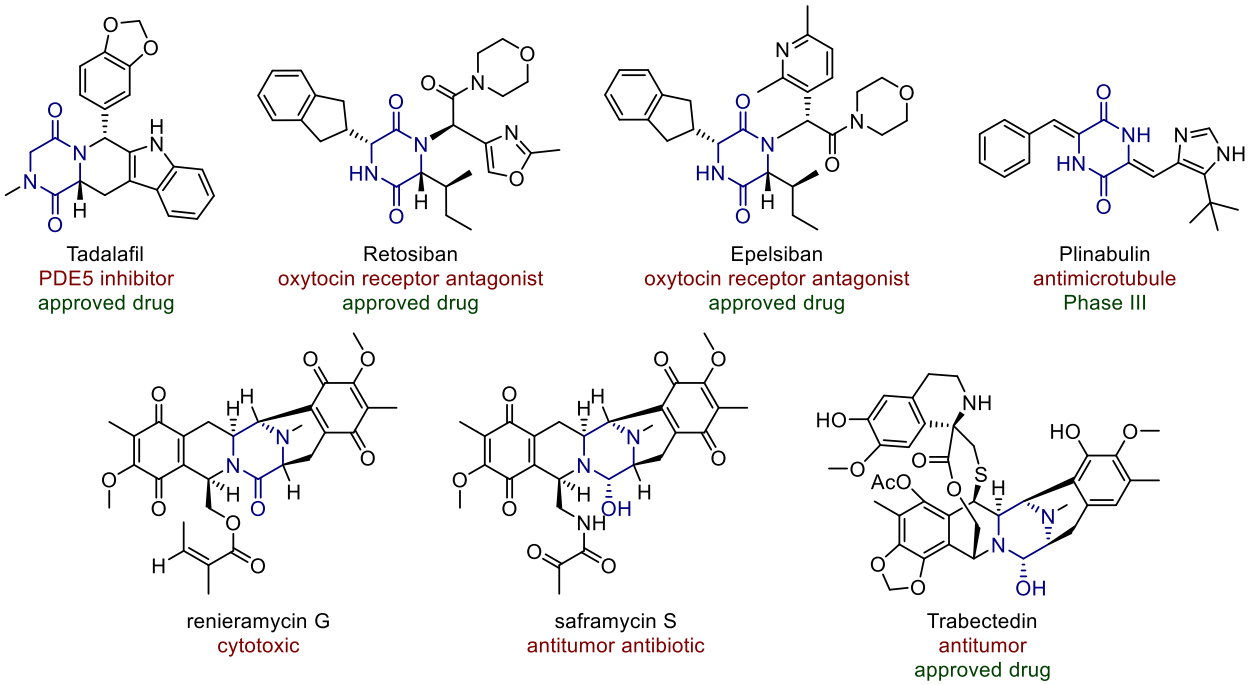

Numerous methods already exist for manipulating the DKP ring which, combined with the low cost and commercial availability of simple DKPs, make complex synthetic targets viable through derivatization.[34,35] The aldol condensation is one well-precedented reaction for derivatizing the methylenes in the DKP ring into alkylidenes, beginning from the inexpensive, commercially available bis-acetoxy DKP **6** and involving simple methodologies. Several bases and conditions have already been extensively explored in the literature for DKP aldol condensations with a variety of aromatic aldehydes†. The DKP aldol condensation with aromatic aldehydes is notable for its ease of execution and reliable results. The aliphatic aldol condensation, on the other hand, has received limited attention, as will be discussed later.

†In the context of this paper, "aromatic aldehyde" and "aromatic aldol condensation" refer to aldehydes whose α-C's are part of aromatic systems; "aliphatic aldehyde" and "aliphatic aldol condensation", conversely, refer to those with non-aromatic α-C's, even if the aldehyde contains an aromatic moiety.

Three downsides accompany the aldol condensation:

1) Iterative aldol condensations occur unintentionally to produce symmetric bis-condensation alkylidenes. However, the iterative condensations are mostly controllable using exact stoichiometric ratios. The bis-condensation product usually constitutes only a small percentage of the crude product

anyway, and it should generally be chemically distinct enough from the mono-condensation product to enable separation.

2) Protection/deprotection rounds are necessary when either the aldehyde or DKP contains protons more acidic than the CH_2. The CH_2, as the site of enolization, is an integral part of the aldol condensation mechanism shown in Scheme 3, and deprotonation elsewhere can interfere with the desired pathway. However, protection/deprotection is not necessary for a single condensation and for substrates devoid of acidic protons.

3) Strong bases like KOtBu and elevated temperatures are commonly utilized to effect the transformation. This limits the aldol condensation's practicability in the synthesis of delicate or complex molecules. However, the use of acetoxy DKPs facilitates elimination with the acyl transfer shown in Scheme 3 and enables the use of mild conditions and bases.

Scheme 3. Acetoxy DKP aldol condensation mechanism.

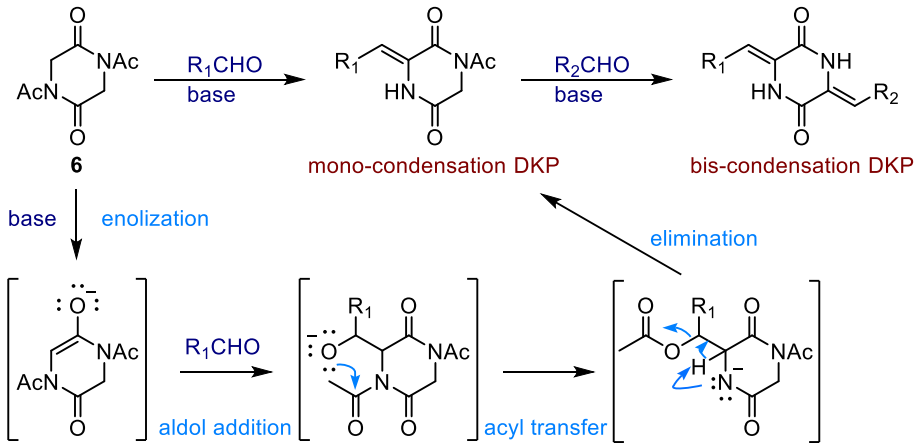

Despite the proliferation of aldol condensation precedents for acetoxy DKPs with aromatic aldehydes, few examples of aliphatic aldol condensations are available and fewer still involve acetoxy DKPs. Most DKPs with aliphatic side-arms are constructed via cyclization of glycine derivatives.[35] This restricts the feasibility of certain targets, requires carefully tailored reaction conditions, and makes the production of derivatives laborious. It is not clear why the aldol condensation has not been used more often to introduce aliphatic moieties as it has for aromatics and why strong bases are employed instead of acetoxy DKPs and mild conditions. Our search for literature examples of DKP aldol condensations with aliphatic aldehydes yielded 26 unique molecules used by a handful of groups (shown in Figure 3) according to SciFinder and Reaxys database searches and self-guided investigation. The parameters for the database searches are shown in Figure 4.

These substrates possess notably inert hydrocarbon structures with few functional groups among them. The bolded names indicate groups which condensed the aldehydes onto an acetoxy DKP in mild conditions (i.e. Cs_2CO_3, DBU, rt) while the italicized denote acetoxy DKPs in harsh conditions (i.e. KOtBu, NaH, heat) and the unaffected names did not use acetoxy DKPs. Condensations with aliphatic aldehydes could provide more direct access to targets and broaden the range of substituents possible, especially if they can proceed under mild conditions and preserve pre-existing, delicate functionalities. To investigate this possibility while creating a synthetic route to barettin, we undertook to explore the aliphatic aldol

condensation with functionalized aldehydes; we specifically began with an intrinsically unstable aldehyde (**9**) that would enable direct access to barettin to test the limits of the reaction. If the aliphatic aldol condensation with an acetoxy DKP could work with an aldehyde prone to degradation, then it should theoretically work for any "tamer" replacement.

Figure 3. Aldehydes with non-aromatic α-C's which have undergone DKP aldol condensations.[18,39,40,41,42,43,44,45,46,47,48,49,50,51,52]

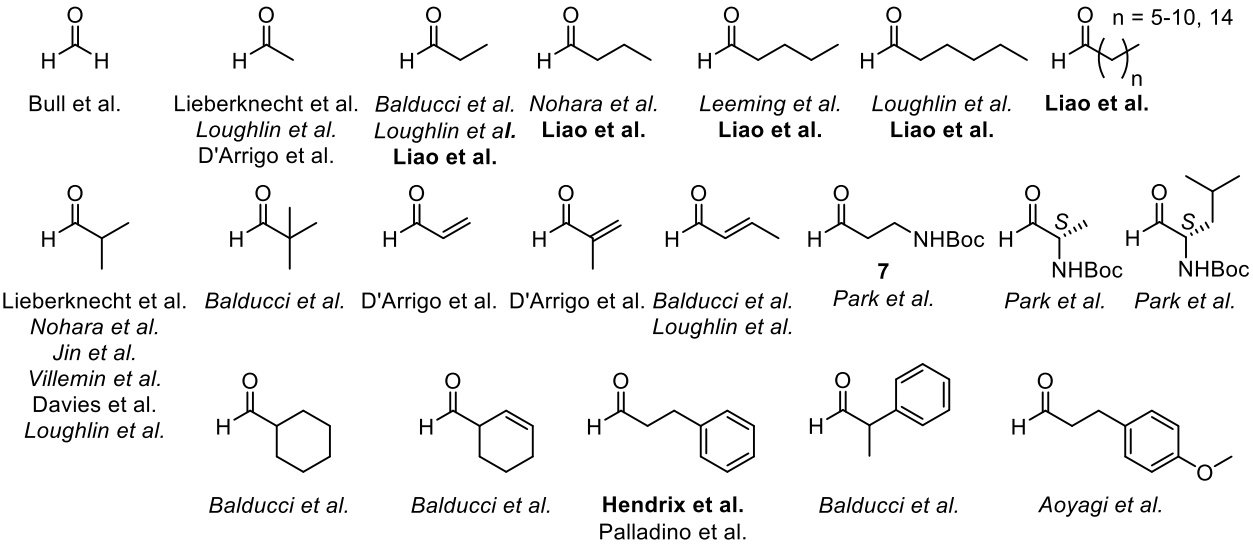

Figure 4. Reaxys and SciFinder search parameters for DKP aldol condensations.

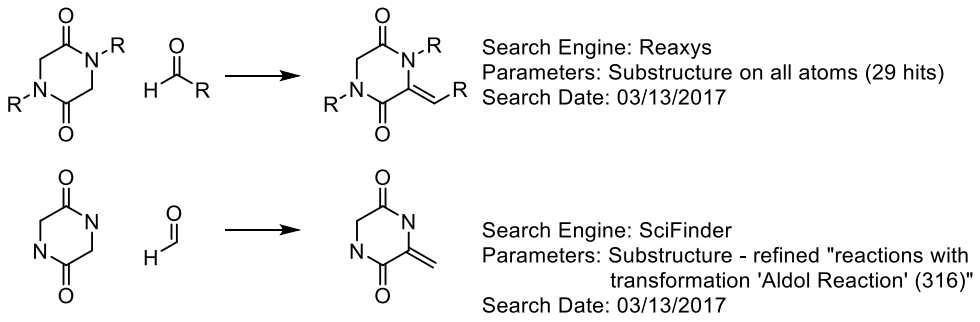

The successful employment of such a method is discussed herein in the context of a total synthesis of barettin which we hope enables large-scale production and rapid development of derivatives both in the barettin and in the overall DKP families. In developing the route, we aimed to address two issues simultaneously: improving the synthetic access to barettin in a manner amenable to derivatization and validating the feasibility of the aliphatic aldol condensation with a sensitive substrate.

Results and Discussion.

We successfully synthesized (±)-(*Z*)-barettin with 31 % yield as a mono-TFA salt over seven steps with only one chromatographic separation (Scheme 4). The route utilized two DKP aldol condensations, the first with an aliphatic aldehyde and the second with an aromatic aldehyde. In this route, we were able to display the feasibility of using a degradation-prone aldehyde to effect an aldol condensation and to

showcase the applicability of the aldol condensation to directly access bioactive scaffolds. The ability of the route to run with a sensitive substrate and with one chromatographic separation over seven steps sets it apart from most total syntheses and should improve its scale-up value. The route is also inherently amenable to alteration to conveniently produce derivatives for SAR studies as shown in Scheme 5, not including the many additional derivatizations possible outside of this specific route. Three major difficulties were encountered over the development of this route: 1) aldehyde **9** and DKP **10** degrade in basic conditions, on silica, and above room temperature; 2) a rearrangement of **12** (Schemes 8 and 9) competes with the second aldol condensation; and 3) desired products **12** and **14** and undesired byproducts **15** (Scheme 8) and **16** (Scheme 10) are not amenable to separation from each other by flash column chromatography.

Scheme 4. Synthetic route to barettin.

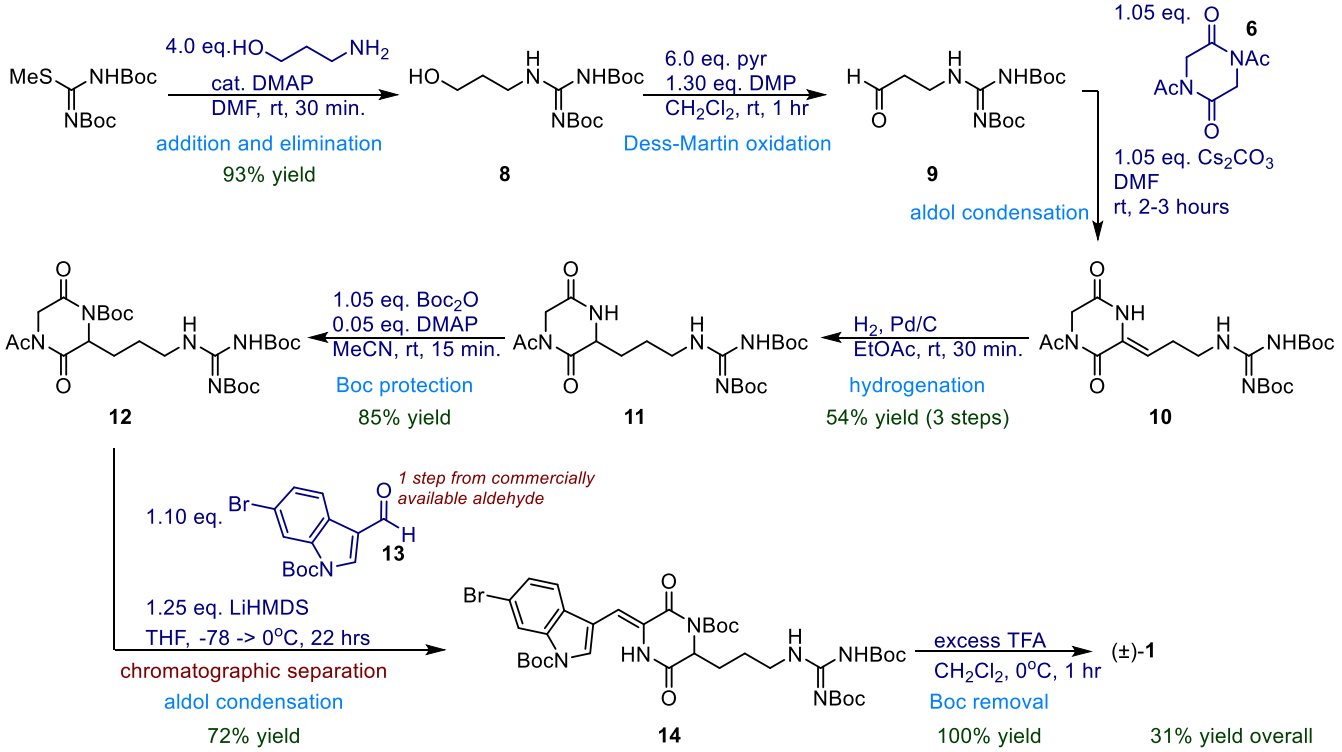

Scheme 5. Amenability of the DKP aldol condensation to produce barettin derivatives for SAR studies.

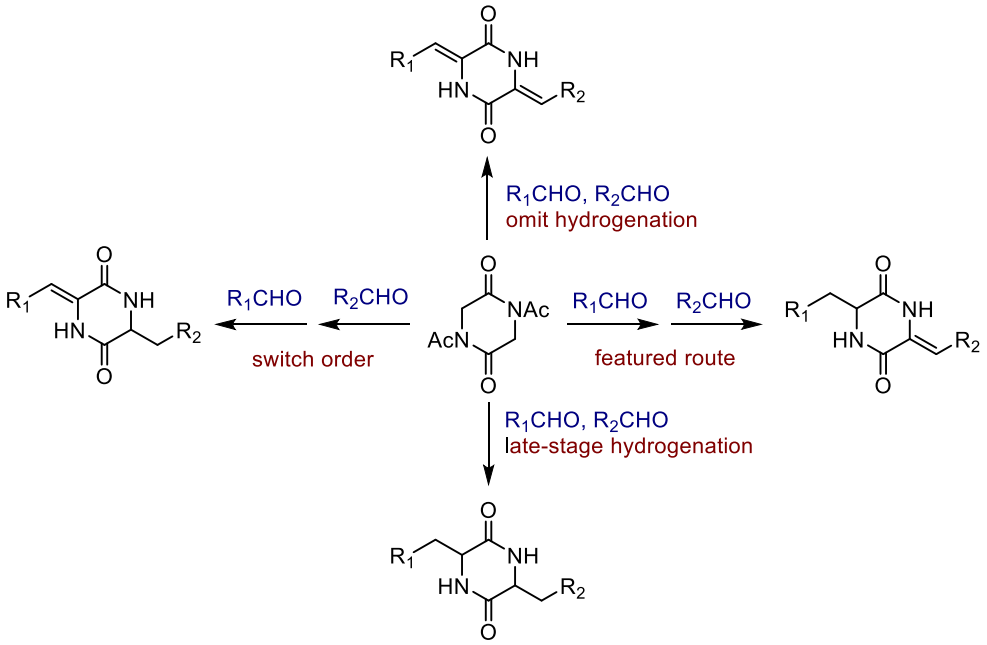

*The first aldol condensation: degradation of **9** and **10**.*

At the project's conception, we anticipated possible degradation of **9** and **10** due to the ability of the guanidino group to eliminate. The position of a π bond three atoms away from the guanidino would lower the pKa of the allylic hydrogen and further encourage elimination according to our proposed mechanism (Schemes 6 and 7). Accordingly, serious degradation was encountered on silica gel, in basic conditions, and with heat. When both **9** and **10** were exposed to 60 °C, neither were recovered. Surprisingly, both compounds can be dried under reduced pressure in a hot water bath at 40 °C and appear stable to store in excess of a week at 0 °C. We also observed that the aldol condensation's yields suffered when allowed to run overnight and that excess **6** was recovered despite the use of equivalent amounts of **6** and **9**. This suggested that **9** and **10** degraded over time in the basic conditions of the aldol condensation.

Scheme 6. Proposed mechanism for guanidino elimination in basic conditions.

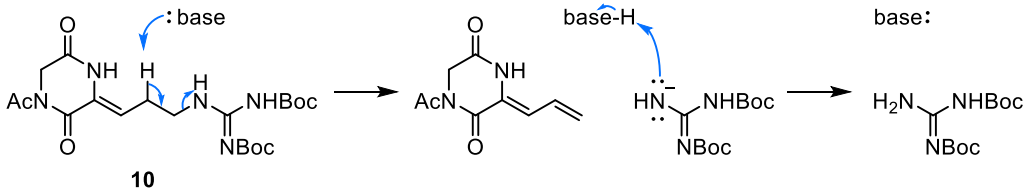

Scheme 7. Proposed mechanism for guanidino elimination in acidic conditions.

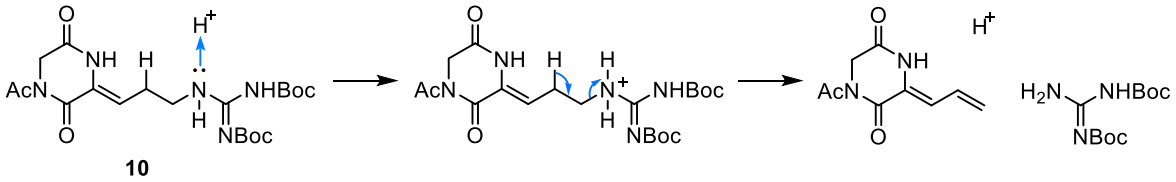

Attempted purification of **9** or **10** on silica caused % recovery to plunge (Table 1), and the desired products continued to elute off the column in mixed fractions long after the bulk of the pure material had been collected. Due to these difficulties, we decided to subject **10** to the hydrogenation before attempting chromatographic purification since the loss of the π bond makes elimination less favorable. However, we were unsure how to handle the purification of **9**: the aldol condensation produced its highest estimated yield when pure **9** was utilized, yet the aldehyde suffered serious recovery losses on silica during the purification. We therefore attempted to optimize the Dess-Martin oxidation to eliminate the need for pyridine (which was the only significant impurity after work-up of **9**), but attempts at using different bases or less pyridine led to impractically impure and low-yielding results.

*Table 1. Recovery losses from using flash column chromatography to purify **9** and **10** on silica.*

Entry	Compound	Estimated **9**/**10** pre-column† (mg)	**9**/**10** recovered post-column (mg)	Estimated % recovery
1	**9**	55	32	58
2	**9**	406	142	35
3	**10**	24	12	50.
4	**10**	39	14	36
5	**10**	115	40	35
6	**10**	172	60	35
7	**10**	224	23	10.
8	**10**	349	206	59
9	**10**	1,079	227	21

†Pre-column amounts of **9** and **10** are inflated by presence of residual pyridine and DMF; however, these residual solvents do not account for all the lost mass.

We therefore determined to subject **9** to the condensation with the residual pyridine because purification of **9** on silica led to a worse overall yield than did the "dirty" aldol condensation: we therefore ran the alcohol **8** through the Dess-Martin oxidation all the way to the hydrogenation without any chromatographic purification. As predicted, **11** was perfectly amenable to chromatographic separation, neither degrading nor trailing on the column. Serendipitously, however, we found that chromatographic purification of **11** was not even necessary as the only remaining impurity was excess **6** from the aldol condensation (which is removed in downstream purification and does not participate in subsequent reactions). We propose that either hydrogenation reduced the minor byproducts from the oxidation and aldol condensation into volatile species or that the carbon backbone for the palladium catalyst adsorbed the impurities and therefore removed them from the mixture during filtration. Whatever the cause, we achieved the route from **8** to **11** in 54 % yield without any chromatographic separation as seen in Scheme 4.

*The second aldol condensation: rearrangement of **12** into **15**.*

During the second aldol condensation between DKP **12** and aromatic aldehyde **13**, an interesting rearrangement of **12** into **15** was observed by ^{1}H NMR spectroscopy. Contrary to our expectations, the sterically hindered methine in the DKP ring underwent enolization when treated to certain bases, resulting in a ring contraction that excludes the neighboring amide group from the ring. We propose that this ring contraction proceeds according to the mechanism reported by Farran and co-workers who observed base-induced ring contractions for doubly-Boc protected DKPs.[53] Our proposed analogous mechanism is represented in Scheme 9. This competing rearrangement led to lower yields and separation issues since **12**, **14**, and **15** were not amenable to separation by flash column chromatography. Fortunately, we completely bypassed this rearrangement and its associated issues by experimenting with different conditions; of the many variations tested, the most efficacious alterations were changes in base and temperature, as shown in the abbreviated Table 2. Using 1.25 equivalents of LiHMDS (Table 2, entry 5), we secured very good yields of **14** with complete consumption of **12**, no formation of **15**, and a reliable separation from excess aldehyde **13**.

Scheme 8. Competition between second aldol condensation and rearrangement.

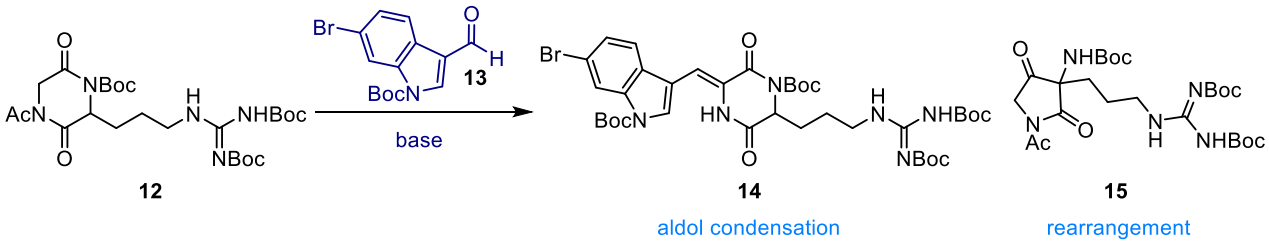

*Scheme 9. Farran & co-worker's TRAL (transannular rearrangement of activated lactams) mechanism applied to **12**.*

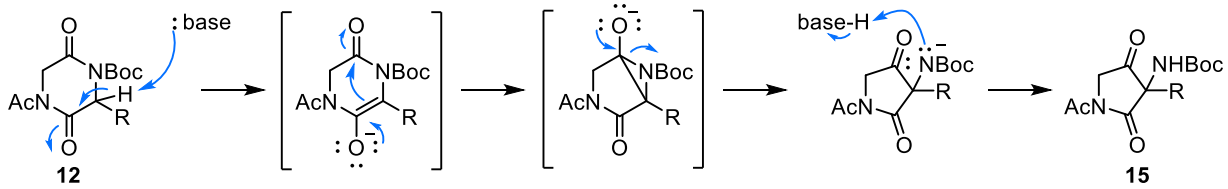

Table 2. Optimization of the second aldol condensation.

Entry	Base	Equivalence to **12**	Temperature (°C)	**14 : 15**
1	Cs_2CO_3	1.1	Rt	0 : 100
2	DBU	1.0	Rt	14 : 86
3	DBU	1.0	0	33 : 67
4	LiHMDS	1.0	-78 -> 0	100 : 0 Incomplete rxn
5	LiHMDS	1.25	-78 -> 0	100 : 0 72 % yield
6	LiHMDS	2.0	-78 -> 0	No rxn

*Boc-acylation of **12**: a separation issue.*

Surprisingly, the Boc protection of **11** presented a real challenge, despite the universal practice of using Boc anhydride to protect amides. DMAP is a mild base, yet it appears to enolize the unsubstituted methylene of **12** which then attacks the Boc anhydride to produce Boc-acylated **16** (Scheme 10). The presence of **16** is minor, usually less than 10 % of the overall isolated product. However, it leads to serious separation difficulties downstream since all our efforts to develop chromatographic conditions to separate **16** from **12** and **14** were ineffective. We therefore optimized the reaction conditions of the Boc protection to minimize formation of **16**. As DMAP, excess Boc anhydride, and time increased, not only did the production of **16** increase and the % yield of **12** decrease but the results also became more irreproducible. Using only 0.05 equivalents of DMAP (the smallest amount we could weigh), 1.05 equivalents of Boc anhydride, and closely monitoring the reaction by TLC gave reproducible results with 0-2 % formation of **16** and very good yield (85 %) for the desired transformation.

*Scheme 10. Boc protection of **11** and proposed acylation of **12**.*

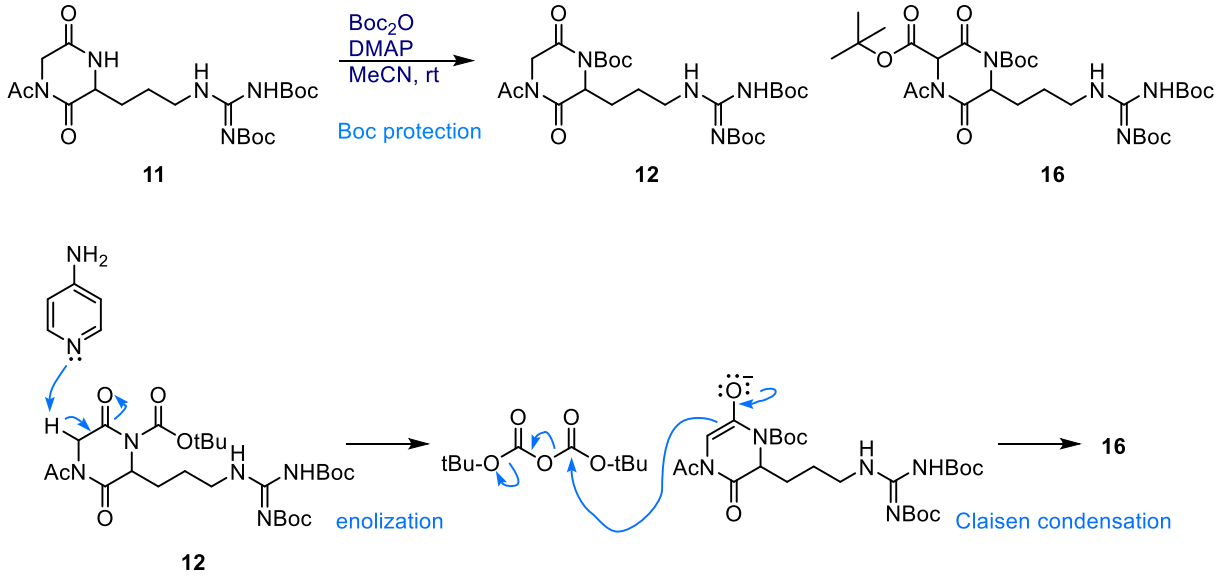

Conclusion.

The previous synthesis of (*Z*)-barettin reported 13 % yield over five steps, with multiple chromatographic separations. We synthesized (±)-(*Z*)-barettin with 31 % yield as a mono-TFA salt over seven steps with only one chromatographic separation. The route is efficient, proceeds under mild conditions, and is optimized to reduce formation of undesired byproducts otherwise seen in the aldol condensations and the Boc protection. Our route enables us to 1) utilize a DKP condensation with an unstable aliphatic aldehyde, 2) showcase how the DKP condensation provides direct access to a bioactive scaffold, and 3) suggest a simple, higher yielding route to barettin and analogues consisting of only one chromatographic separation.

Future Directions.

We plan to continue exploring the aliphatic aldol condensation while engaging in bioassay-guided derivatization of **1** and while attempting to access other bioactive DKP scaffolds using this methodology.

We will test the bioactivity of our racemic barettin to determine if the stereochemistry affects potency; if it does, we will alter the route to selectively hydrogenate. We also plan to generate derivatives for biological study as well.

Due to the difficulties encountered with the guanidino moiety, we are currently subjecting a simpler amino aldehyde (**7**) to the same synthetic route (Scheme 11) and will test its efficacy against barnacle settlement to determine whether the guanidino moiety is necessary for activity. We hope that the terminal amino group will possess a reduced potential to eliminate and be more amenable to the basic conditions of the aldol condensation as well as the acidic conditions of silica chromatography; one precedent exists for this reaction with **7** and tBuOK.[50] If a simpler aldehyde like **7** can be used in place of the degradation-prone **9**, this finding could greatly simplify the production of barettin derivatives**.** The guanidino moiety, which is positively charged under most physiological conditions, likely helps with cellular penetration, but quaternary ammonium compounds are also used as biocides in the food industry and comprise essential endogenous amines such as serotonin and dopamine.[12] The removal of the guanidino group may not alter cellular penetration or activity at all and thus ease synthetic preparation of barettin derivatives.

*Scheme 11. Retrosynthetic plan for modified barettin with amino aldehyde **7**.*

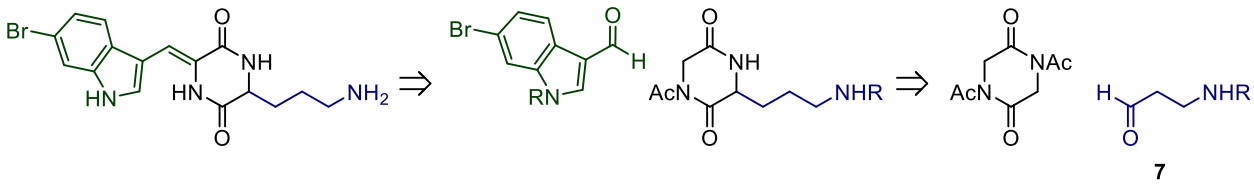

Contact Information.

Elizabeth Wells Kelley at ewkelley@email.wm.edu.

Abbreviations.

Boc = *tert*-butyloxycarbonyl
Boc_2O = di-*tert*-butyl dicarbonate
DBU = 1,8-diazabicyclo[5.4.0]undec-7-ene
DKP = diketopiperazine
DMAP = 4-(dimethylamino)-pyridine
DMF = dimethylformamide
DMP = Dess-Martin periodinane
EtOAc = ethyl acetate
LiHMDS = hexamethyldisilazane lithium salt
MeCN = acetonitrile
Pyr = pyridine
Rt = room temperature (approximately 23 ^{o}C)
TFA = trifluoroacetic acid
THF = tetrahydrofuran

Experimental.

All reactions were carried out under N_2 atmosphere and room temperature with magnetic stirring in dried reaction vessels unless otherwise indicated. Acetonitrile and tetrahydrofuran were anhydrous, degassed with argon and

purified by passage through a column of molecular sieves and a bed of activated alumina.[54] All reagents were used as received unless otherwise noted. Analytical thin layer chromatography was performed on SiliCycle 60Å glass plates. Flash column chromatography was conducted with silica gel (230-400 mesh).[55] Visualization was accomplished with UV light and a stain, followed by heating. Melting points were obtained on a Mel-Temp II. Film infrared spectra were recorded using a Shimadzu IRTracer-100 FTIR spectrophotometer and are reported in cm^{-1}. ^1H NMR spectra were recorded on an Agilent VnmrJ 4 (400 MHz) spectrometer and are reported in ppm using solvent as an internal standard ($CDCl_3$ at 7.26 ppm and DMSO at 2.50 ppm) or tetramethylsilane (0.00 ppm) unless otherwise noted. Proton-decoupled ^{13}C NMR spectra were recorded on an Agilent VnmrJ 4 (400 MHz) spectrometer and are reported in ppm using solvent as an internal standard ($CDCl_3$ at 77.00 ppm) unless otherwise noted. All compounds were judged to be homogeneous (>95% purity) by ^1H NMR spectroscopy unless otherwise noted.

8. 1,3-bis(Boc)-2-methyl-2-thiopseudourea (4.00 g, 13.78 mmol) was dissolved in DMF (41.7 mL). 3-aminopropanol (4.14 g, 55.1 mmol) and DMAP (168 mg, 1.38 mmol) were sequentially added. After 1.5 hours, the reaction mixture was diluted with 0.1 M AcOH (80 mL), and the reaction mixture was extracted using Et_2O (3 x 80 mL). The combined organic layers were sequentially washed with saturated $NaHCO_3$ (80 mL), saturated NaCl (80 mL), and H_2O (80 mL). The organic layer was dried over Na_2SO_4 and concentrated under reduced atmosphere to afford alcohol **8** as a white crystalline solid (4.07 g, 12.8 mmol, 93% yield). The spectral data of **8** is in agreement with published literature.[56]

9. Alcohol **8** (2.00 g, 6.30 mmol) and pyridine (3.06 mL, 37.8 mmol) were dissolved in CH_2Cl_2 (11.0 mL). Dess-Martin periodinane (3.48 g, 8.19 mmol) was suspended in CH_2Cl_2 (30.0 mL) in a separate flask. The solution of **8** and pyridine was added to the DMP solution dropwise using a syringe. CH_2Cl_2 (6.0 mL) was used to wash the original **8**-pyridine flask and syringe and add the residues to the reaction mixture. After 1 hour, 1 M NaOH (75 mL, 75 mmol) and Et_2O (30 mL) were added, and the reaction mixture stirred for an additional 10 minutes. The reaction mixture was separated from the aqueous using Et_2O (100 mL), washed with H_2O (3 x 80 mL), dried over Na_2SO_4, and concentrated under reduced atmosphere to afford unpurified aldehyde **9** as a sticky yellow solid with some residual pyridine (1.86 g, 5.89 mmol). The material was used in the subsequent reaction without further purification. A portion of **9** was purified by flash column chromatograph for analytical purposes. The spectral data of **9** is in agreement with published literature.[56]

6. Glycine anhydride (5.00 g, 43.8 mmol) was dissolved in acetic anhydride (20.7 mL, 219 mmol). The reaction flask was fitted with a reflux condenser and heated to 110 ^oC (bath temperature). After 27 hours, the reaction mixture was concentrated under reduced atmosphere to afford bis-acetoxy DKP **6** as a light brown solid (8.64 g, 43.6 mmol, 99.5% yield). The spectral data of **6** is in agreement with published literature.[53]

10. Bis-acetoxy DKP **6** (1.17 g, 5.89 mmol) and aldehyde **9** (1.86 g, 5.89 mmol) were dissolved in DMF (14.2 mL). Following addition of Cs_2CO_3 (2.01 g, 6.18 mmol), the reaction flask was repeatedly evacuated (50 torr) and backfilled with N_2 to remove ambient O_2 from the reaction. After 2 hours, the reaction mixture was diluted with H_2O (150 mL), and the reaction mixture was extracted with EtOAc (4 x 40 mL). A small quantity of saturated NaCl solution was added to mitigate emulsions. The combined organic layers were washed with sat. NaCl, dried over Na_2SO_4, and concentrated under reduced atmosphere to afford mono-condensation DKP **10** as a white solid (2.83 g, 6.23 mmol). The material was used in the subsequent reaction without further purification. A portion of **10** was purified by flash column chromatograph for analytical purposes: TLC in 40% EtOAc/Hex) R_f: 0.46 (UV/CAM); IR (film) 1724, 1685, 1637, 1319, 1279, 1228, 1052, 1020, 775, 731 cm^{-1}; ^1H NMR (400 MHz, $CDCl_3$) 11.48 (s, 1H), 9.10 (s, 1H), 8.52 (t, *J* = 5.5 Hz, 1H), 6.30 (t, *J* = 8.4 Hz, 1H), 4.44 (s, 2H), 3.46 (dt, *J* = 5.9, 8.6 Hz, 2H), 2.60 (s, 3H), 2.57 (dt, *J* = 8.2, 8.7, 2H), 1.50 (s, 9H), 1.48 (s, 9H); ^{13}C NMR (400 MHz, $CDCl_3$) δ 168.5, 159.6, 159.3, 156.0, 152.4, 149.3, 125.4, 115.1, 79.5, 75.9, 42.1, 35.0, 24.2, 24.1, 23.2, 21.9; Exact mass calc'd for $C_{20}H_{31}N_5O_7Na$ $[M + Na]^+$ 476.211569, found 476.211476.

11. Mono-condensation DKP **10** (1.15 g, 2.54 mmol) was dissolved in EtOAc (10.2 mL), and 10% palladium on activated wood carbon (reduced, 50% water wet paste) was added in one portion (500 mg). The reaction mixture was sparged with H_2 for a couple minutes and then left under an H_2 atmosphere for about 45 minutes. The reaction mixture was flushed with Ar and gravity filtered. The filter pad was rinsed with several portions of CH_2Cl_2. The

filtrate was concentrated under reduced atmosphere to afford hydrogenated mono-condensation DKP **11** as an off-white crystalline solid (834 mg, 1.83 mmol, 54% yield over three steps from alcohol **8**): m.p. 203-206 °C; TLC (40% EtOAc in hexanes) R_f: 0.19 (UV/CAM); IR (film) 1730, 1708, 1685, 1650, 1364, 1329, 1271, 1225, 1162, 1134, 1099, 1050, 1024, 980, 740 cm^{-1}; ^1H NMR (400 MHz, $CDCl_3$) 11.41 (s, 1H), 8.45 (t, *J* = 5.9 Hz, 1H), 7.79 (d, *J* = 2.4 Hz, 1H), 4.49 (d, *J* = 18 Hz, 1H), 4.25 (m, 1H), 4.18 (d, *J* = 18 Hz, 1H), 3.51 (ddt, *J* = 6.2. 6.7. 7.0 Hz, 1H), 3.31 (ddt, *J* = 6.2, 6.6, 6.8 Hz, 1H), 2.56 (s, 3H), 1.84 (m, 4H), 1.47 (s, 18H); ^{13}C NMR (400 MHz, $CDCl_3$) δ 171.9, 169.3, 166.4, 166.3, 163.2, 156.6, 153.3, 83.5, 79.9, 79.8, 55.7, 45.7, 38.9, 38.8, 29.8, 28.2, 28.1, 27.3, 24.9†; Exact mass calc'd for $C_{20}H_{33}N_5O_7Na$ $[M + Na]^+$ 478.227220, found 478.227006.

†There were four more carbon peaks observed than expected. Considering that eight of the peaks had a neighboring peak with an extremely similar chemical shift (166.4 vs. 166.3, 79.9 vs. 79.8, 38.9 vs. 38.8, 28.2 vs. 28.1), we propose that we observed a rotamer of **11**.

12. Hydrogenated mono-condensation DKP **11** (100 mg, 0.220 mmol) was dissolved in MeCN (0.88 mL). Boc_2O (49 µL, 0.23 mmol) was added as a liquid, followed by addition of DMAP (1.3 mg, 0.011 mmol). After 17 minutes, the reaction was complete as judged by TLC, and the reaction mixture was diluted with EtOAc (10 mL) and washed sequentially with saturated NH_4Cl (5 mL) and saturated NaCl (5 mL). The organic layer was dried over Na_2SO_4 and concentrated under reduced atmosphere to afford Boc-hydrogenated mono-condensation DKP **12** as a white crystalline powder (103 mg, 0.186 mmol, 85% yield): m.p. 53-59 °C; TLC (40% EtOAc in hexanes) R_f: 0.53 (UV/CAM); IR (film) 1782, 1714, 1637, 1613, 1574, 1367, 1131, 727 cm^{-1}; ^1H NMR (400 MHz, $CDCl_3$) 11.48 (s, 1H), 8.36 (s, 1H), 5.05 (d, *J* = 18.8 Hz, 1H), 4.82 (t, *J* = 7.6 Hz, 1H), 3.97 (d, *J* = 18.4 Hz, 1H), 3.47 (m, 2H), 2.58 (s, 3H), 1.90 (m, 2H), 1.74 (m, 2H), 1.54 (s, 9H), 1.48 (s, 18H); ^{13}C NMR (400 MHz, $CDCl_3$) δ 171.3, 167.9, 164.0, 163.7, 156.4, 153.5, 150.1, 85.4, 83.5, 79.5, 60.1, 46.6, 39.9, 30.1, 28.4, 28.2, 28.0, 27.2, 25.8; Exact mass calc'd for $C_{25}H_{41}N_5O_9Na$ $[M + Na]^+$ 578.279649, found 578.279508.

13. 6-bromo-1*H*-indole-3-carboxaldehyde (778 mg, 3.47 mmol) was dissolved in MeCN (10 mL). Boc_2O (0.82 mL, 3.8 mmol) was added as a liquid, followed by addition of DMAP (13 mg, 0.10 mmol). After half an hour, the reaction mixture was concentrated under reduced pressure. The residue was dissolved in EtOAc (40 mL) and washed sequentially with saturated $NaHCO_3$ (3 x 20 mL) and saturated NaCl (2 x 20 mL). The organic layer was dried over Na_2SO_4 and concentrated under reduced pressure to afford aldehyde **13** as a flaky coral solid (1.11 g, 3.41 mmol, 98% yield). The spectral data of **13** is in agreement with published literature.[57]

14. A dry flask was charged with Boc-hydrogenated mono-condensation DKP **12** (50. mg, 0.090 mmol). The atmosphere was flushed with N_2, and the flask was kept under an unbroken N_2 atmosphere for all subsequent steps. In a separate flask, aldehyde **13** (32 mg, 0.099 mmol) was dissolved in THF (0.26 mL) under a N_2 atmosphere. DKP **12** was dissolved in THF (0.30 mL) and cooled at -78 °C for fifteen minutes, after which 1.0 M LiHMDS (113 µL, 0.113 mmol) was added. Five minutes after the addition of LiHMDS, all of the **13** solution was added to the flask containing **12**. The flask and syringe were rinsed with additional THF (0.23 mL). Twenty minutes after adding **13**, the flask was transferred to an ice bath and kept at 0 °C for an hour. The flask was then allowed to warm to rt overnight. 22 hours after beginning the procedure, the reaction was quenched with saturated NH_4Cl (15 mL) and extracted with EtOAc (2 x 15 mL). The combined organic layers were washed with saturated NaCl (30 mL), dried over Na_2SO_4, and concentrated under reduced pressure. The resulting residue was purified by flash column chromatography (0 % -> 10 % EtOAc/$CHCl_3$) to afford Boc-barettin **14** as a yellow crystalline solid (53 mg, 0.065 mmol, 72% yield): TLC (10% EtOAc in $CHCl_3$) R_f: 0.44 (UV/CAM); IR (film) 1714, 1638, 1616, 1366, 1228, 1146, 1131, 726 cm^{-1}**;** ^1H NMR (400 MHz, $CDCl_3$) 11.44 (s, 1H), 8.32 (m, 2H), 8.12 (br s, 1H), 7.88 (s, 1H), 7.48 (d, *J* = 8.2 Hz, 1H), 7.41 (dd, *J* = 1.8, 8.5 Hz, 1H), 7.22 (d, *J* = 1.2 Hz, 1H), 4.78 (t, *J* = 7.1 Hz, 1H), 3.44 (dt, *J* = 7.1, 13 Hz, 2H), 1.93 (m, 2H), 1.68 (m, 2H), 1.66 (s, 9H), 1.55 (s, 9H), 1.44 (s, 9H), 1.41 (s, 9H); ^{13}C NMR (400 MHz, $CDCl_3$) δ 166.3, 163.6, 159.1, 156.2, 153.2, 151.0, 148.8, 135.7, 128.3, 126.9, 125.8, 125.5, 120.4, 119.5, 118.7, 113.4, 110.5, 85.7, 84.7, 83.1, 79.3, 58.6, 40.0, 31.9, 28.3, 28.1, 28.0, 25.2; Exact mass calc'd for $C_{37}H_{51}BrN_6O_{10}H$ $[M + H]^+$ 819.292281, found 819.292415.

(±)-1•HO_2CCF_3 (barettin•HO_2CCF_3). Boc-barettin **14** (34 mg, 0.041 mmol) was dissolved in anhydrous CH_2Cl_2 (0.91 mL). The reaction mixture was cooled to 0 °C and sparged with argon. TFA (0.91 mL, 11 mmol) was added. After stirring for 1 hour at 0 °C, the reaction mixture warmed to rt and was concentrated under reduced pressure to afford mono-TFA barettin **(±)-1• HO_2CCF_3** as a flaky yellow solid (22 mg, 0.042 mmol, 100% yield). The spectral data of **(±)-1** is in agreement with published literature with minor differences (Table 3, entries 1 and 18).[19,58]

Figure 5. Numbering scheme for Table 3.

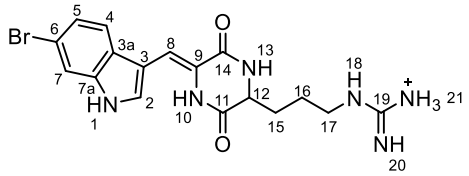

*Table 3. ^1H and ^{13}C NMR data of (±)-**1**• HO_2CCF_3 in DMSO-d_6 compared to Solter and co-workers†.[19]*

Entry‡	Type	^{13}C δ (ppm)		^1H δ (ppm)		*J* (Hz)	
1	NH	---	---	12.12	11.77	d, *J* = 2.5	s
2	aromatic	127.45	126.46	7.99	7.95	d, *J* = 2.5	d, *J* = 2.4
3	aromatic	109.87	107.44	---	---	---	---
3a	aromatic	127.55	127.73	---	---	---	---
4	aromatic	120.87	120.44	7.62	7.60	d, *J* = 8.5	d, *J* = 8.6
5	aromatic	224.52*	123.51	7.24	7.23	dd, *J* = 1.6, 8.5	dd, *J* = 1.9, 8.6
6	Br & aromatic	117.03	115.16	---	---	---	---
7	aromatic	115.69	114.83	7.67	7.62	d, *J* = 1.6	d, *J* = 2.0
7a	aromatic	138.42	137.00	---	---	---	---
8	alkene	110.95	108.58	6.99	6.96	s	s
9	alkene	123.35	123.18	---	---	---	---
10	NH	---	---	9.63	9.63	s	s
11	C=O	168.61	167.14	---	---	---	---
12	CH	56.48	55.11	4.07	4.04	m	m
13	NH	---	---	8.45	8.38	d, *J* = 2.5	d, *J* = 2.4
14	C=O	163.36	161.17	---	---	---	---
15	CH_2	32.62	31.67	1.76-1.84	1.74	m	m
16	CH_2	25.11	24.48	1.50-1.63	1.55	m	m
17	CH_2	41.98	obscured by DMSO	3.16-3.20	3.11	m	dt, *J* = 6.7, 12.9
18	NH	---	---	8.01	7.44	t, *J* = 6.0	m
19	C=N	158.61	157.12	---	---	---	---
20/21	NH/NH_3^+	---	---	7.00-7.78	7.5-6.4	br	br

†The values on the left in split cells are data reported by Solter and co-workers. The values on the right in split cells are our data.
‡We are following the numbering scheme outlined by Solter and co-workers.
*We believe the original paper had a typo and meant to express the ^{13}C chemical shift of C-5 as 124.52 ppm.

Acknowledgements.

This work was carried out at the College of William & Mary in Williamsburg, Virginia from Fall semester 2016 to Spring semester 2017. I would like to express my utmost gratitude to Professor Jonathan Scheerer for his

dedication in advising and mentoring me throughout my undergraduate research career and the graduate school application process,

to my labmate Skylar Norman for assisting me in this project by running the first six, painful iterations of the first aldol condensation,

to Jonathan Perkins for his helpful guidance and practical advice in the lab, and

to all my instructors who imparted the foundational skills and knowledge necessary for research and a career in chemistry.

References.

[1] C. M. Magin, S. P. Cooper, and A. B. Bernnan (2010). Non-toxic antifouling strategies, *Materials Today, 13*(4), 36-44.
[2] International Maritime Organization (2002). Anti-fouling systems, 1-31.
[3] Fusetani (2003). Biofouling and antifouling, *Natural Products Reports, 21*, 94-104.
[4] Yebra, Kiil, and Dam-Johansen (2004). Antifouling technology – past, present, and future steps towards efficient and environmentally friendly antifouling coatings, *Progress in Organic Coatings, 50,* 74-104. DOI: 10.1016/j.porgcoat.2003.06.001.
[5] A. Abbott, P. D. Abel, D. W. Arnold, and A. Milne (2000). Cost-benefit analysis of the use of TBT: the case for a treatment approach, *The Science of the Total Environment, 258*, 5-19.
[6] D. Pimentel, L. Lach, R. Zuniga, and D. Morrison (2000). Environmental and economic costs of nonindigenous species in the United States, *BioScience, 50*(1), 53-65.
[7] Dafforn, Lewis, and Johnston (2011). Antifouling strategies: History and regulation, ecological impacts, and mitigation, *Marine Pollution Bulletin, 62*, 453-465. DOI: 10.1016/j.marpolbul.2011.01.012.
[8] Transparency Market Research (October 30, 2015). *Flourishing Shipbuilding Industry in Asia Pacafic Drives Demand for Marine Coatings, Global Market to be worth US$11.8 bn by 2020* [Press release]. Retrieved from http://www.transparencymarketresearch.com/pressrelease/marine-coatings.htm (accessed April 10, 2017).
[9] Photos obtained from http://www.european-coatings.com/Homepage-news/Nanotechnology-and-anti-fouling, https://us.v-cdn.net/5019629/uploads/editor/0h/gpxipr4ligdj.jpg, and http://news.nationalgeographic.com/news/2010/01/100119-viking-shipwrecks-worms-shipworms-global-warming/, respectively.
[10] Almeida, Diamantino, and de Souda (2007). Marine paints: The particular case of antifouling paints, *Progress in Organic Coatings, 59*, 2-20. DOI: 0.1016/j.porgcoat.2007.01.017.
[11] International Maritime Organization (2001). Adoption of the final act of the conference and any instruments, recommendations, and resolutions resulting from the work of the conference, *International Convention on the Control of Harmful Anti-Fouling Systems on Ships, 2001*, 1-26.
[12] Gule, Begum, and Klumperman (2015). Advances in biofouling mitigation: A review, *Critical Reviews in Environmental Science and Technology, 46*(6), 535-555. DOI: 10.1080/10643389.2015.1114444.
[13] Intertanko, Guide to Modern Antifouling Systems & Biofouling Management, 1st ed. (2016).
[14] K. V. Thomas and S. Brooks (2009). The environmental fate and effects of antifouling paint biocides, *Biofouling, 26*(1), 73-88. DOI: 10.1080/08927010903216564.
[15] Hellio, Marechal, Gama, Pereira, and Clare (2009). "Natural marine products with antifouling activities". *Advances in Marine Antifouling Coatings and Technologies*. Woodhead Publishing. Retrieved from http://researchgate.com. DOI: 10.1533/9781845696313.3.572.
[16] Lidgren, Bohlin, and Bergman (1986). Studies of Swedish marine organisms VII, *Tetrahedron Letters, 27*(28), 3283-3284.
[17] Sjogren, Goransson, Johnson, Dahlstrom, Andersson, Bergman, Jonsson, and Bohlin (2004). Antifouling activity of brominated cyclopeptides from the marine sponge *Geodia barretti, Journal of Natural Products, 67*, 368-372.
[18] Lieberkecht and Griesser (1987). What is the structure of barettin?, *Tetrahedron Letters, 28*(37), 4275-4278.
[19] Solter, Dieckmann, Blumenberg, and Francke (2002). Barettin, revisited?, *Tetrahedron Letters, 43*, 3385-3386.
[20] Johnson, Bergman, Sjogren, and Bohlin (2004). Synthesis of barettin, *Tetrahedron, 60*, 961-965.

[21] M. Sjogren, M. Dahlstrom, U. Goransson, P. R. Jonsson, and L. Bohlin (2004). Recruitment in the field of *Balanus improvises* and *Mytilus edulis* in response to the antifouling cyclopeptides barettin and 8,9-dihydrobarettin from the marine sponge *Geodia barretti*, *Biofouling, 20*(6), 291-297. DOI: 10.1080/08927010400027027.
[22] Lind, Hansen, Osterud, Eilertsen, Bayer, Engqvist, Leszczak, Jorgensen, and Andersen (2013). Antioxidant and anti-inflammatory activities of barettin, *Marine Drugs, 11*, 2656-2666.
[23] Hedner, Sjogren, Frandberg, Johansson, Goransson, Dahlstrom, Jonsson, Nyberg, and Bohlin (2006). Brominated cyclopeptides from the marine sponge *Geodia barretti* as selective 5-HT ligands, *Journal of Natural Products, 69*, 1421-1424.
[24] Olsen, Hansen, Moodie, Isaksson, Sepcic, Cergolj, Svenson, and Andersen (2016). Marine AChE inhibitors isolated from *Geodia barretti*: Natural compounds and their synthetic analogues*, Organic & Biomolecular Chemistry., 14*, 1629-1640.
[25] Yamamoto, Shimizu, Tachnibana, and Fusetani (1999). Roles of dopamine and serotonin in larval attachment of the barnacle *Balanus Amphitrite, Journal of Experimental Zoology, 284*, 746-758.
[26] Sjogren, Johnson, Hedner, Dahlstrom, Goransson, Shirani, German, Jonsson, and Bohlin (2006). Antifouling activities of synthetic peptide analogs of the sponge metabolite barettin, *Peptides, 27*, 2058-2064.
[27] Hedner, Sjogren, Hodzic, Andersson, Goransson, Jonsson, and Bohlin (2008). Antifouling activity of a dibrominated cyclopeptide from the marine sponge *Geodia barretti, Journal of Natural Products, 71*, 330-333.
[28] Sjogren, Jonsson, Dahlstrom, Lundalv, Burman, Goransson, and Bohlin (2011). Two brominated cyclic dipeptides released by the coldwater marine sponge *Geodia barretti* act in synergy as chemical defense, *Journal of Natural Products, 74*, 449-454.
[29] Firn and Jones (2000). The evolution of secondary metabolism – a unifying model, *Molecular Microbiology, 37*(5), 989-994.
[30] Bergman (2013). Synthesis & studies of two marine indole alkaloids, barettin & caulersin, *Phytochem. Rev, 12*, 487-494.
[31] J. H. Andersen, E. Hansen, K.-E. Eilertsen, K. F. Lind, B. Oesterud, and T. Hofer. U.S. Patent Application 20,160,039,796, 2016.
[32] R. Matusch, H.-R. Hofmann, B. Asmussen, and A. Koch. U.S. Patent Application 20,110,311,593, 2011.
[33] J. Bergman, L. Bohlin, M. Sjogren, and U. Goransson. U.S. Patent Application 20,090,124,634, 2009.
[34] C. J. Dinsmore and D. C. Beshore (2002). Recent advances in the synthesis of diketopiperazines, *Tetrahedron, 58*, 3297-3312.
[35] Borthwick (2012). 2,5-diketopiperazines: Synthesis, reactions, medicinal chemistry, and bioactive natural products, *Chemical Reviews, 112*, 3641-3716.
[36] Huang, Zhou, Xu, Yang, and Liu (2010). Diketopiperazines from marine organisms, *Chemistry & Biodiversity, 7*, 2809-2829.
[37] M. B. Martins and I. Carvalho (2007). Diketopiperazines: biological activity and synthesis, *Tetrahedron, 63*, 9923-9932. DOI: 10.1016/j.tet.2007.04.105.
[38] S. Rajappa and M. V. Natekar (1993). Piperazine-2,5-diones and related lactim ethers, *Advances in Heterocyclic Chemistry, 57*, 187-289. DOI: 10.1016/S0065-2725(08)60889-2.
[39] S. D. Bull, S. G. Davies, A. C. Garner, and M. D. O'Shea (2001). Conjugate additions of organocuprates to a 3-methylene-6-isopropyldiketopiperazine acceptor for the asymmetric synthesis of homochiral α-amino acids, *Journal of the Chemical Society, Perkin Transactions 1*, 3281-3287. DOI: 10.1039/b108621a.
[40] P. Leeming, F. R. Fronczek, D. J. Ager, and S. A. Laneman (2000). Asymmetric hydrogenations of diketopiperazines, *Topics in Catalysis, 13*, 175-177.
[41] H. Aoyagi, F. Horike, A. Nakagawa, S. Yokote, N. Park, Y. Hashimoto, T. Kato, and N. Izumiya (1986). Synthesis of unusual aromatic L-amino acids by asymmetric hydrogenation of cyclic dehydrodipeptides, *Bulletin of the Chemical Society of Japan, 59*(1), 323-324.
[42] S.-R. Liao, X.-C. Qin, Z. Wang, D. Li, L. Xu, J.-S. Li, Z.-C. Tu, Y. Liu (2016). Design, synthesis, and cytotoxic activities of novel 2,5-diketopiperazine derivatives, *European Journal of Medicinal Chemistry, 121*, 500-509. DOI: 10.1016/j.ejmech.2016.06.002.
[43] S. Nohara, K. Sawaki, E. Yanase, and S. Nakatsuka (2004). Efficient synthesis of di- and tripeptides containing dehydroamino acids, *ITE Letters on Batteries, New Technologies, and Medicine, 5*(4), 373-376.
[44] S. Jin, P. Wessig, and J. Liebscher (2000). Unusual C=C bond migration in 3-ylidene-2,5-piperazinediones, *European Journal of Organic Chemistry*, 1993-1999.

[45] D. Balducci, P. A. Conway, G. Sapuppo, H. Muller-Bunz, and F. Paradisi (2012). Novel approach to the synthesis of aliphatic and aromatic α-keto acids, *Tetrahedron, 68*, 7374-7379. DOI: 10.1016/j.tet.2012.06.078.
[46] M. C. D'Arrigo, G. Porzi, and S. Sandri (1995). Stereochemical investigation of aldol condensations using (3*R*)- and (3*S*)-3-benzylpiperazine-2,5-dione derivatives, *Journal of Chemical Research (S)*, 430-431.
[47] S. G. Davies, H. Rodriquez-Solla, J. A. Tamayo, A. R. Cowley, C. Concellon, A. C. Garner, A. L. Parkes, and A. D. Smith (2005). Asymmetric conjugate reductions with samarium diiodide: asymmetric synthesis of (2*S*,3*R*)- and (2*S*,3*S*)-[2-^{2}H,3-^{2}H]-leucine[(*S*)-phenylalanine dipeptides and (2*S*,3*R*)-[2-^{2}H,3-^{2}H]-phenylalanine methyl ester, *Organic and Biomolecular Chemistry, 3*, 1435-1447.
[48] D. Villemin and A. B. Alloum (1990). Potassium fluoride on alumina: Condensation of 1,4-diacetylpiperazine-2,5-dione with aldehydes. Dry condensation under microwave irradiation. Synthesis of albonursin and analogues, *Synthetic Communications, 20*(21), 3325-3331. DOI: 10.1080/00397919008051566.
[49] W. A. Loughlin, R. L. Marshall, A. Carreiro, and K. E. Elson (2000). Solution-phase combinatorial synthesis and evaluation of piperazine-2,5-dione derivatives, *Bioorganic & Medicinal Chemistry Letters, 10*, 91-94.
[50] N. G. Park, S. Lee, H. Maeda, H. Aoyagi, and T. Kato (1989). Stereoselective synthesis of 2,4-diamino acids by asymmetric hydrogenation, *Bulletins of the Chemical Society of Japan, 62*, 2315-2319.
[51] J. A. Hendrix, J. T. Strupczewski, K. J. Bordeau, S. Brooks, H. Hemmerle, M. Urmann, X.-Y. Zhao, and P. J. Mueller. U.S. Patent 2,002,066,468, 2002.
[52] M. A. Palladino, G. K. Lloyd, and Y. Hayashi. U.S. Patent Application 20,080,221,122, 2008.
[53] Farran, Parrot, Toupet, Martinez, and Dewynter (2008). Transannular rearrangement of activated 2,5-diketopiperazines: a key route to original scaffolds, *Organic and Biomolecular Chemistry, 6*, 3989-3996. DOI: 10.1039/b810352f.
[54] A. B. Pangborn, M. A. Giardello, R. H. Grubbs, R. K. Rosen, and F. J. Timmers (1996). Safe and convenient procedure for solvent purification, *Organometallics*, *15*, 1518-1520.
[55] W. C. Still, M. Kahn, and A. Mitra (1978). Rapid chromatographic technique for preparative separations with moderate resolution, *Journal of Organic Chemistry, 43*(14), 2923-2925.
[56] Freeman, Tal-Gan, Klein, Levitzki, and Gilon (2011). Microwave-assisted solid-phase aza-peptide synthesis: Aza scan of a PKB/Akt inhibitor using Aza-arginine and Aza-proline precursors, *Journal of Organic Chemistry, 76*, 3078-3085. DOI: 10.1021/jo102422x.
[57] Bentley and Moody (2004). Asymmetric synthesis of the central tryptophan residue of stephanotic acid, *Organic and Biomolecular Chemistry, 2*, 3545-3547. DOI: 10.1039/b414996c.
[58] There is a slight difference in our spectral data compared to Solter and co-worker's, as enumerated in Table 3. However, considering the propensity of NH groups to shift around in proton spectra, the good overlap of all other peaks, and the confirmation of the precursor's structure, we do not consider these differences significant.

Supporting Information.

8 in $CDCl_3$ (400 MHz). 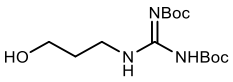

Full-size ^{1}H NMR:

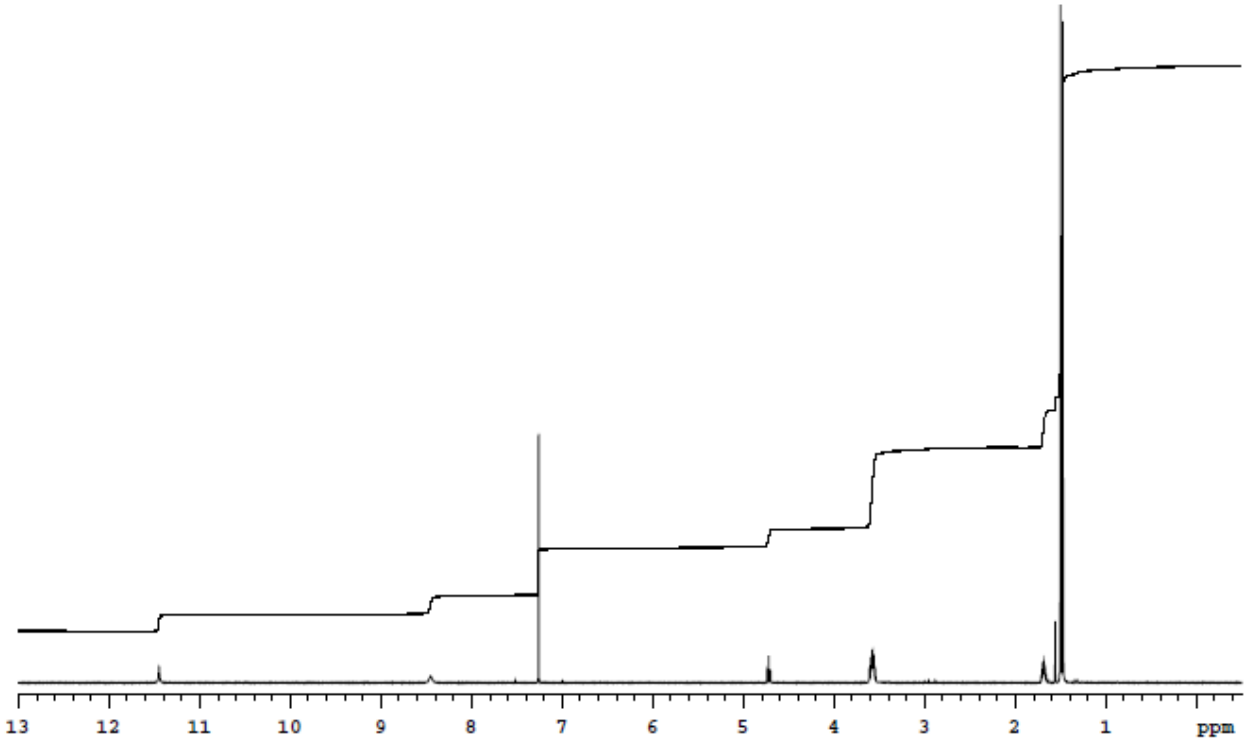

Vertically expanded ^{1}H peaks for clarity:

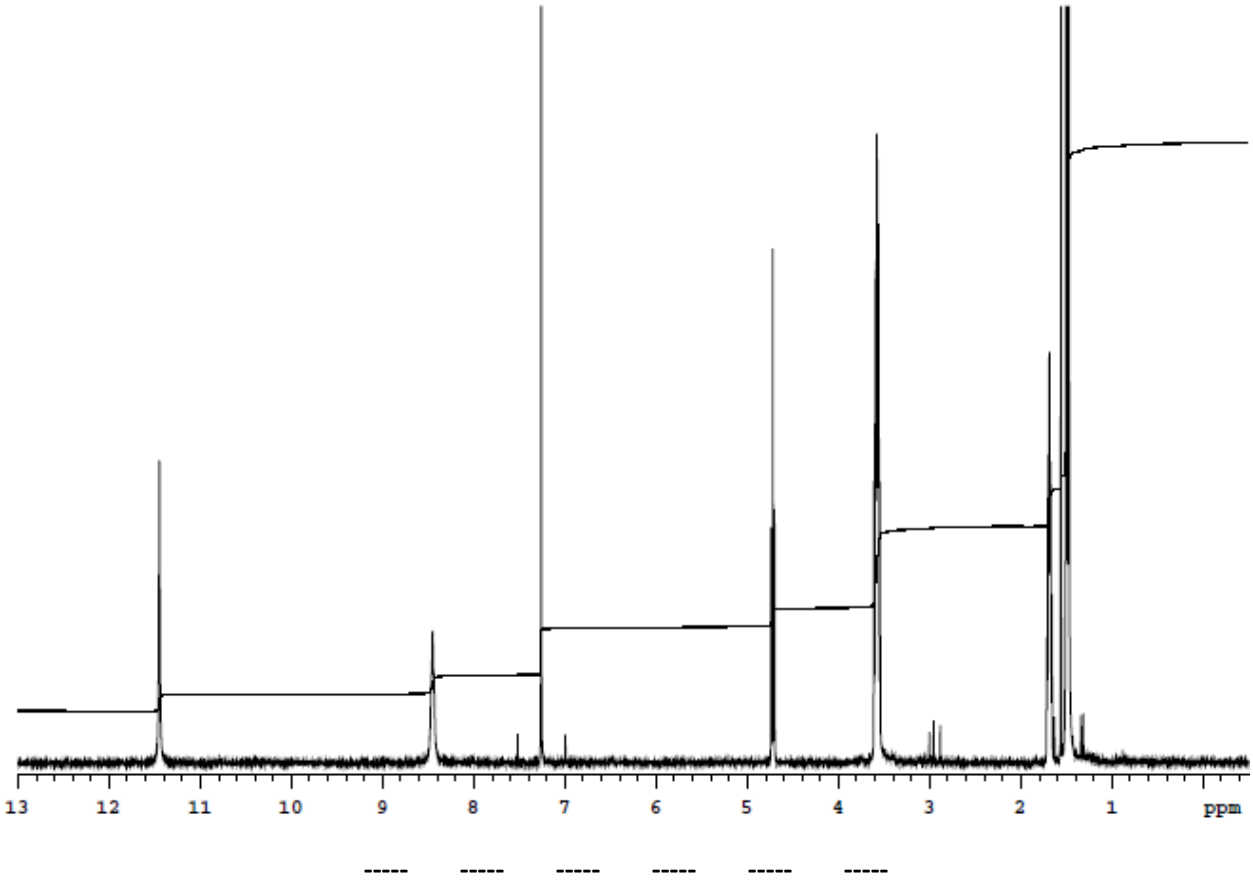

----- ----- ----- ----- ----- -----

9 in $CDCl_3$ (400 MHz). 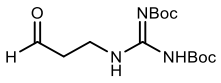

Unpurified full-size ^1H NMR:

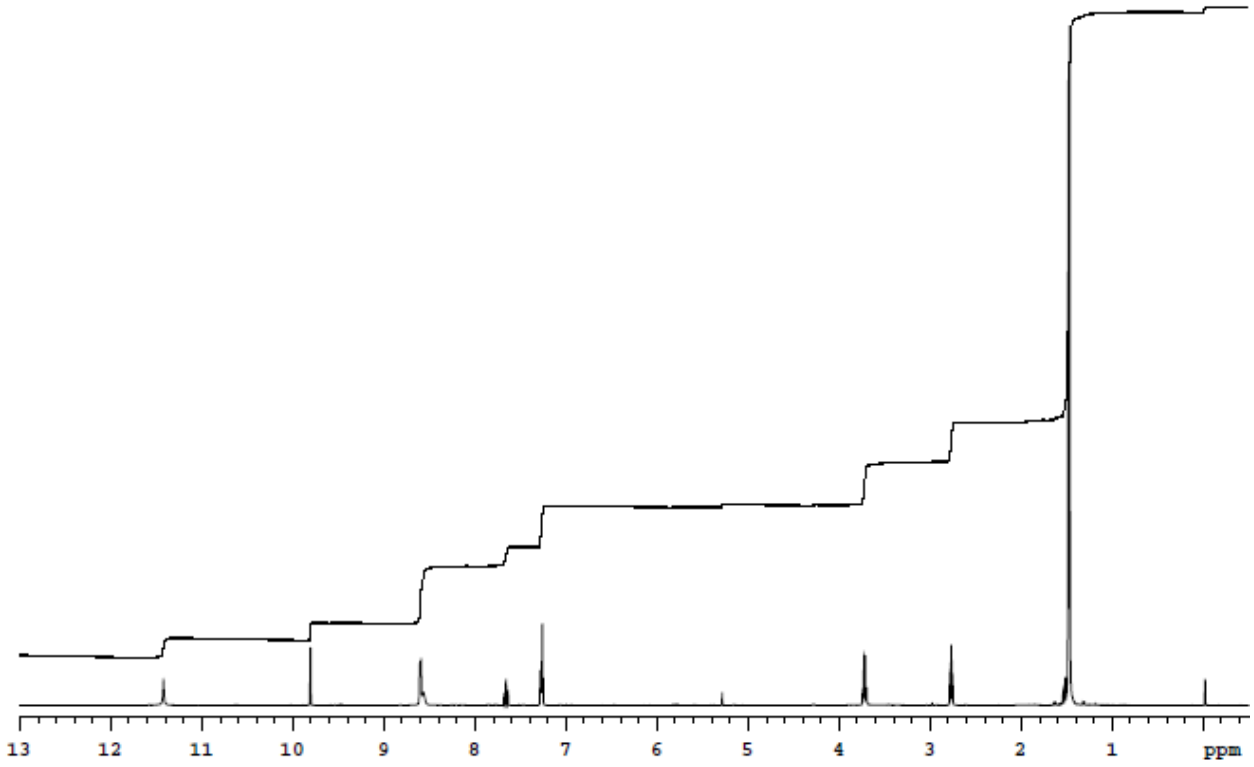

Unpurified vertically expanded ^1H peaks for clarity:

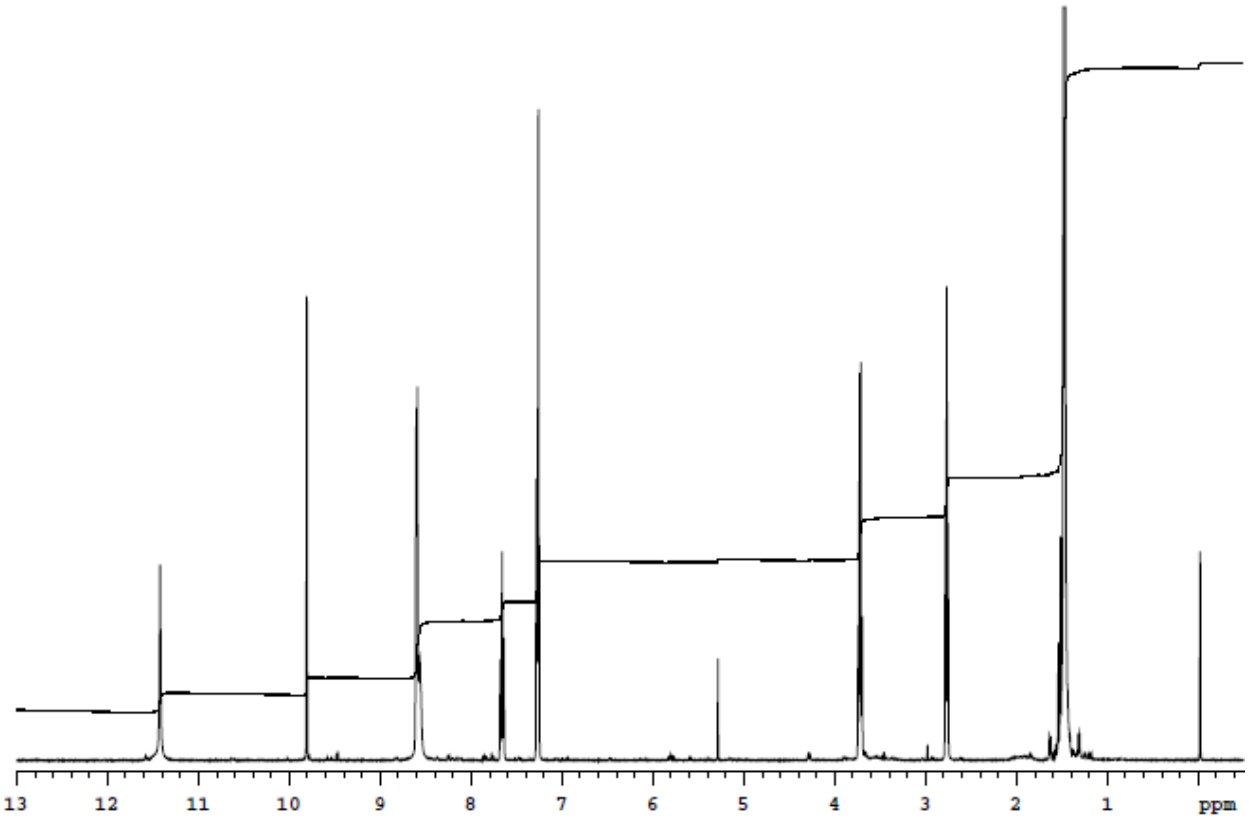

Purified full-size ^{1}H NMR:

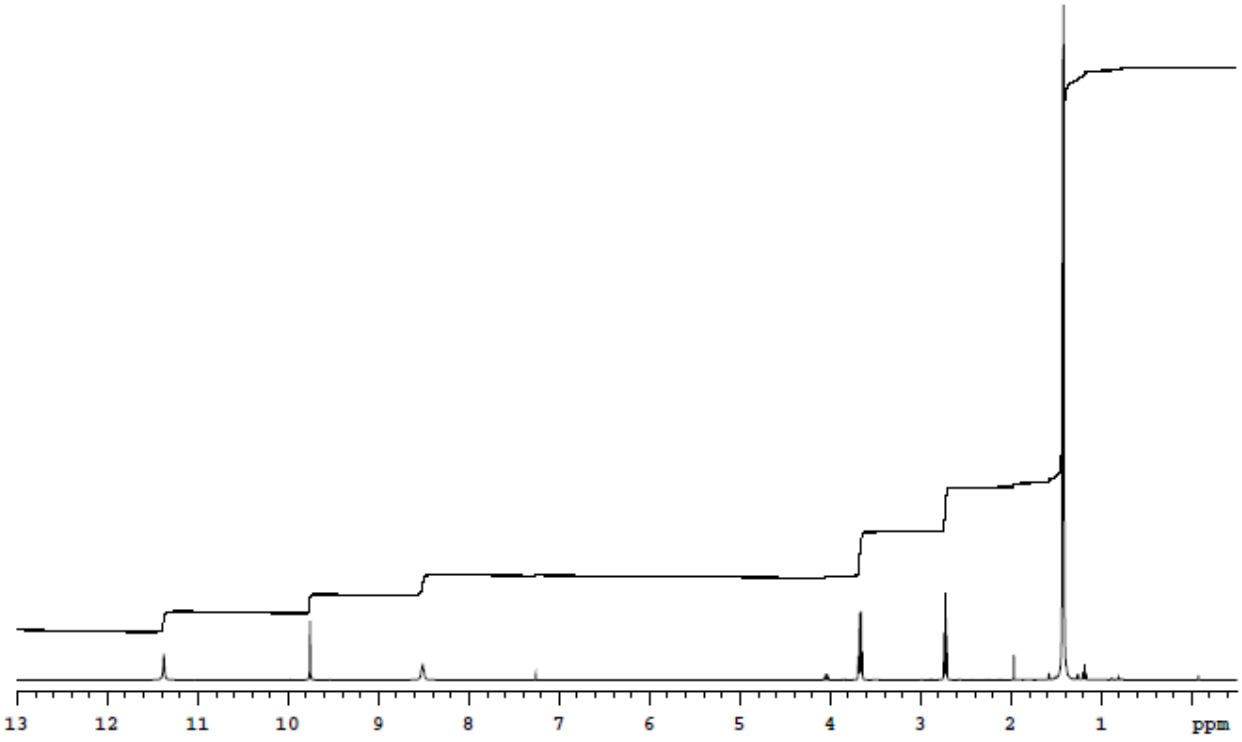

Purified vertically expanded ^{1}H peaks for clarity:

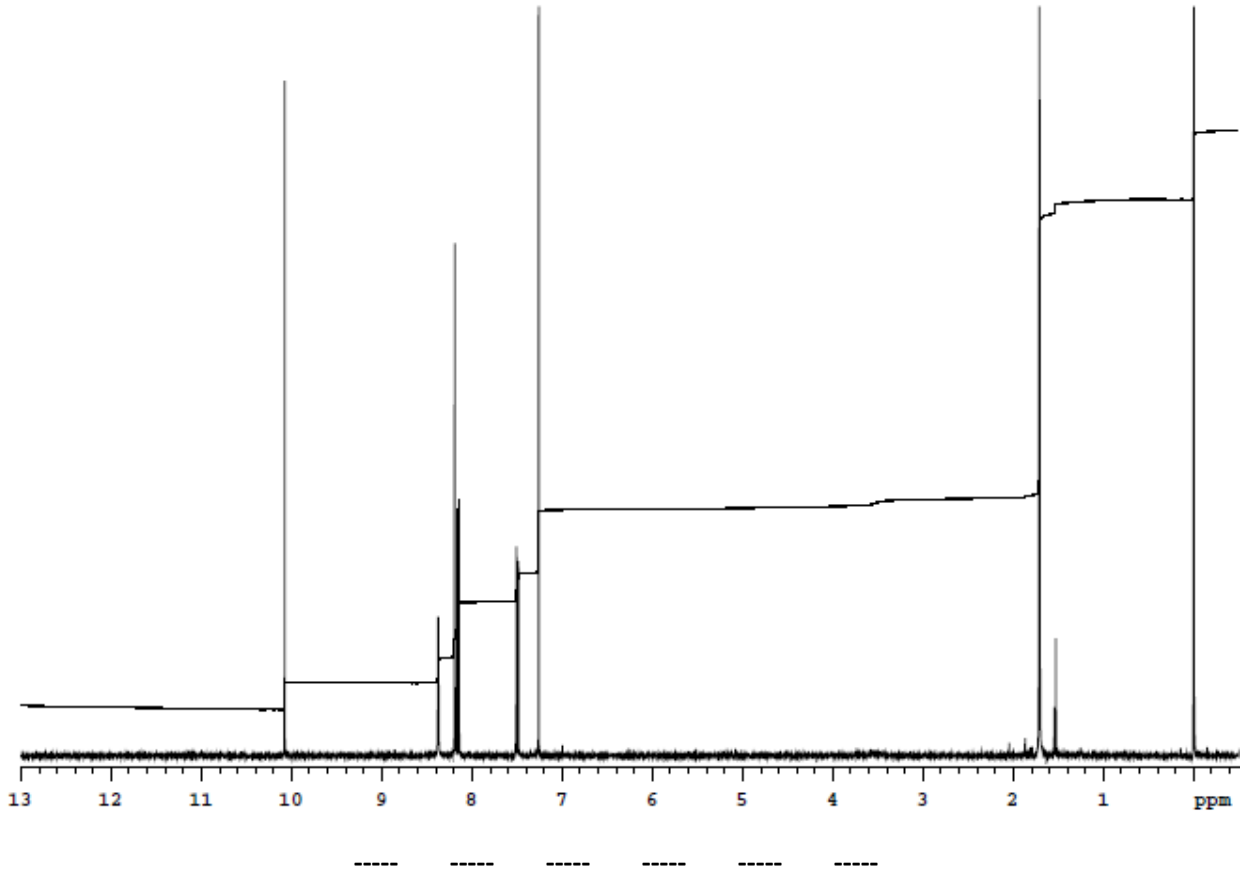

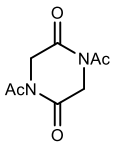

6 in $CDCl_3$ (400 MHz).

Full-size ^{1}H NMR:

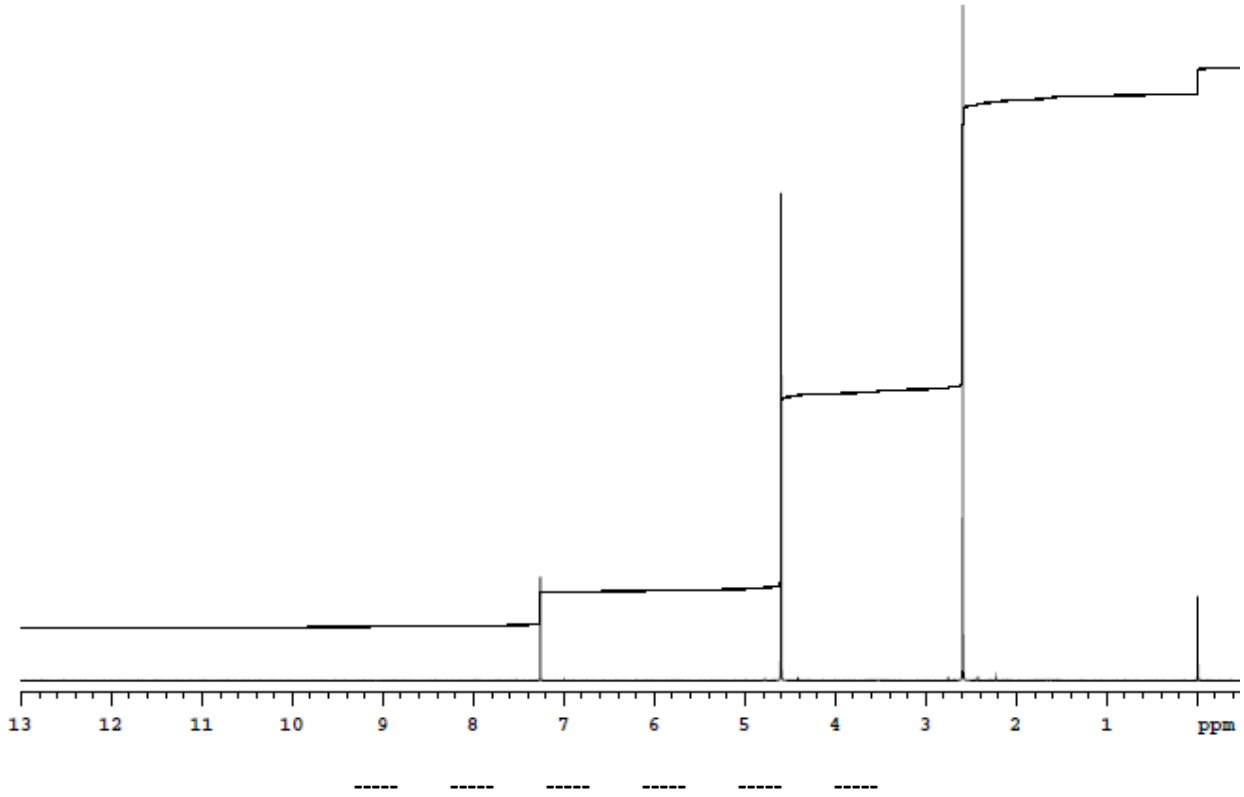

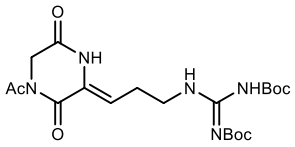

10 in $CDCl_3$ (400 MHz).

Full-size ^1H NMR:

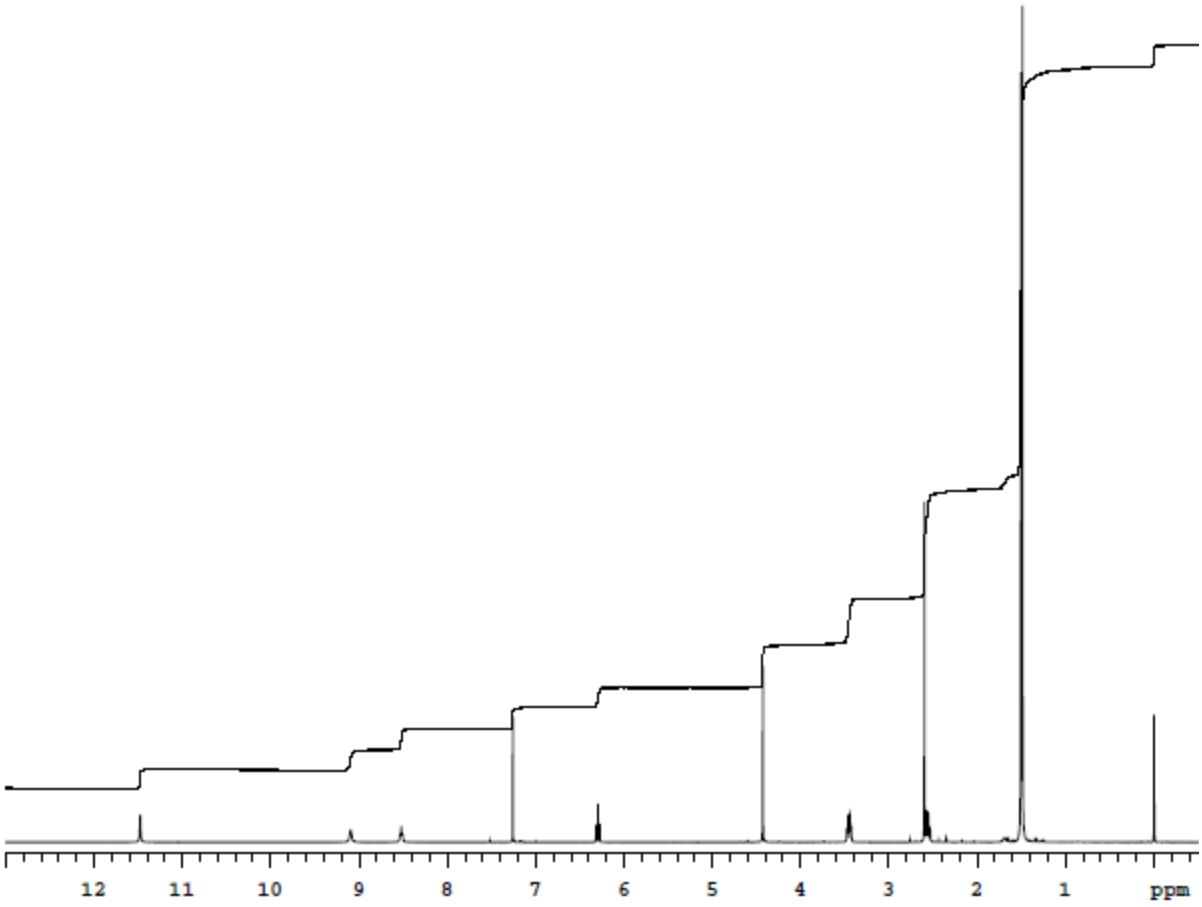

Vertically expanded ^{1}H peaks for clarity:

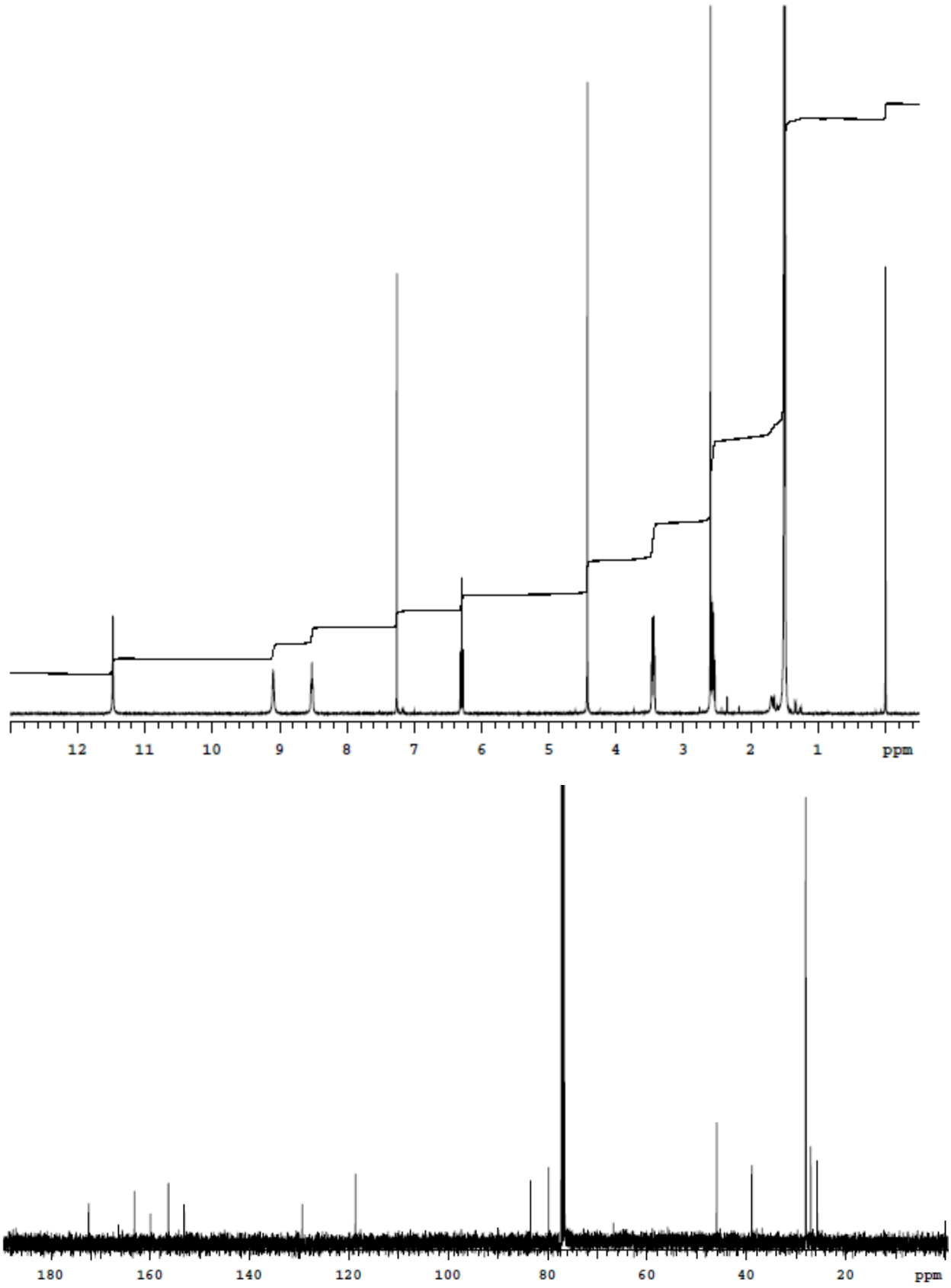
12
11
10
9
8
7
6
5
4
3
2
1
ppm
180
160
140
120
100
80
60
40
20
ppm

----- ----- ----- ----- ----- -----

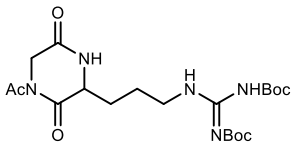

11 in $CDCl_3$ (400MHz).

Full-size ^1H NMR:

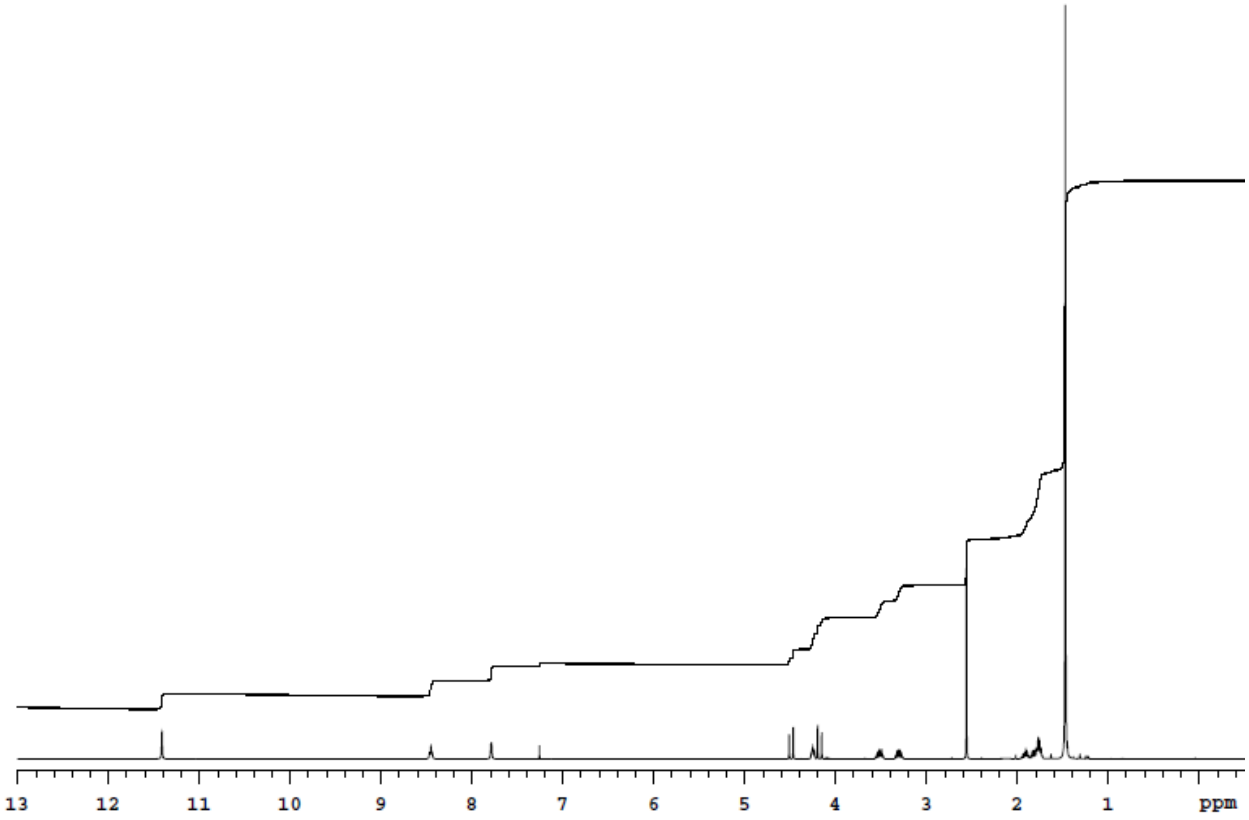

Vertically expanded ^1H peaks for clarity:

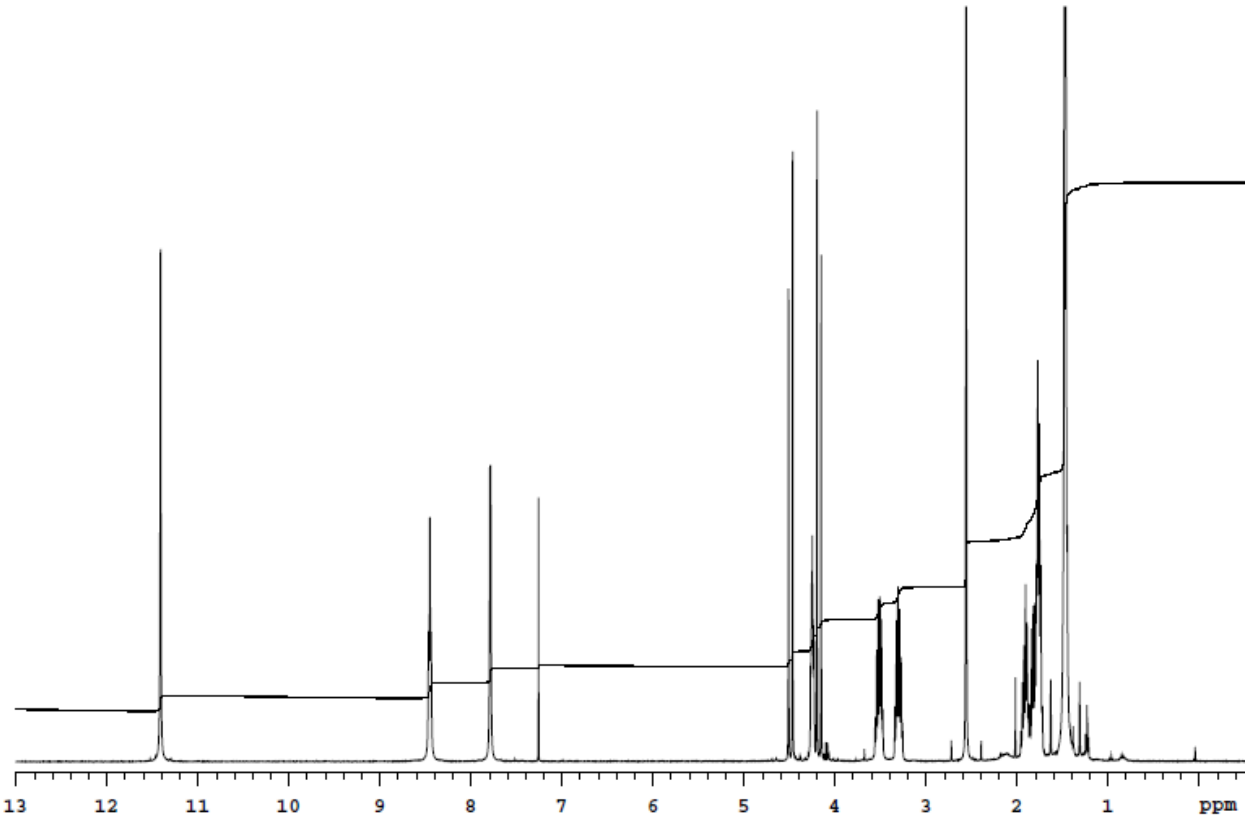
13
12
11
10
9
8
7
6
5
4
3
2
1
ppm

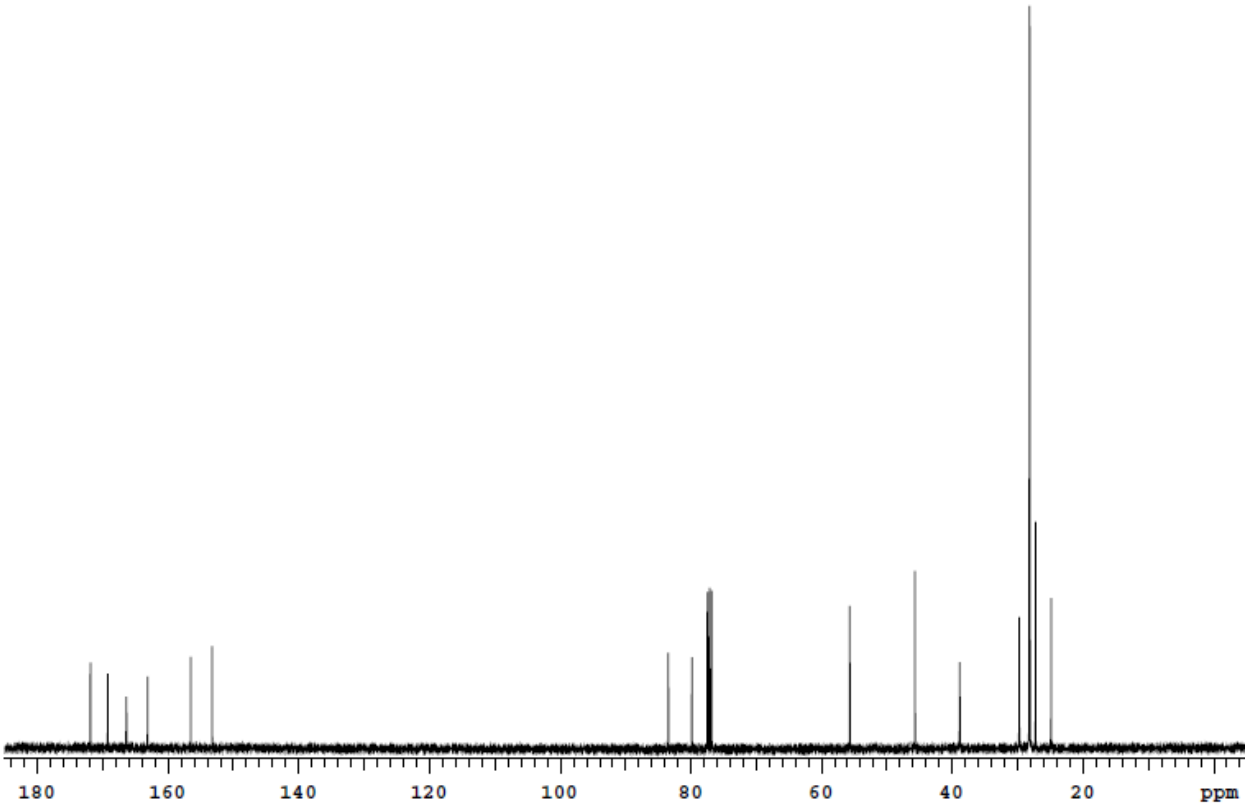
180
160
140
120
100
80
60
40
20
ppm

--- --- --- --- --- ---

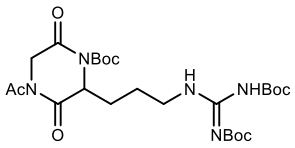

12 in $CDCl_3$ (400 MHz).

Full-size ^1H NMR:

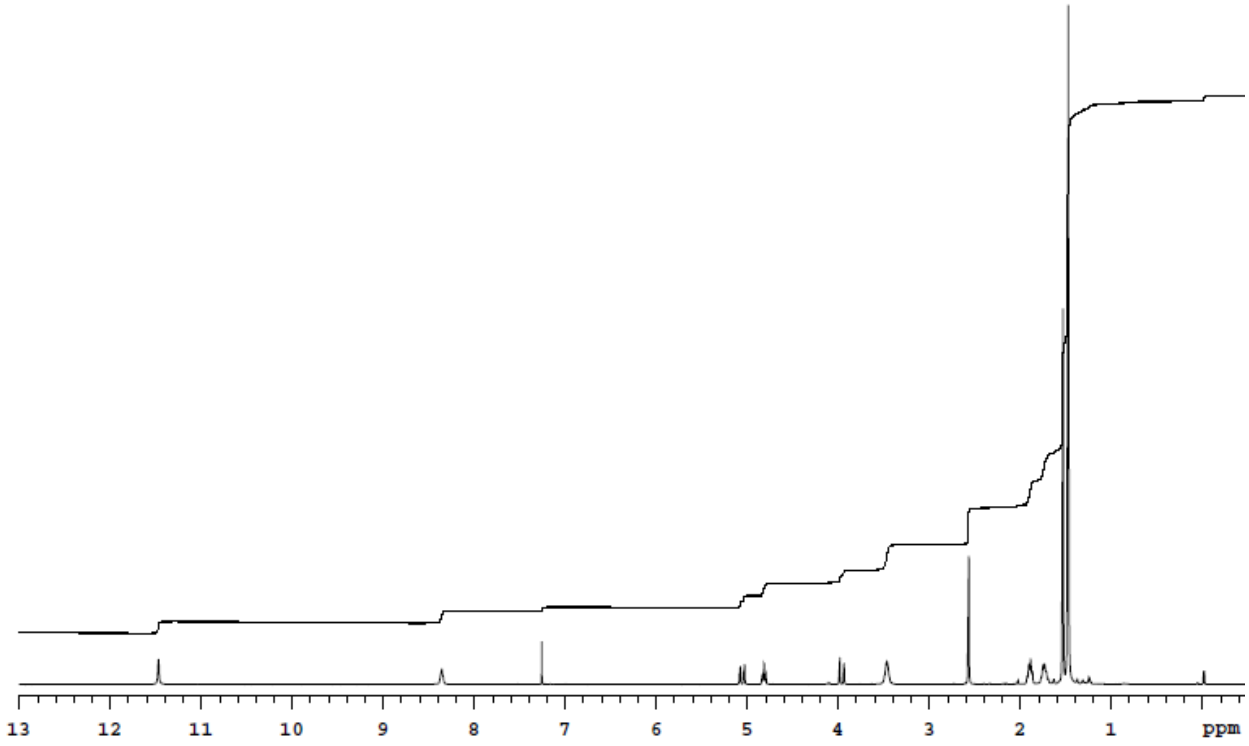

Vertically expanded ^1H peaks for clarity:

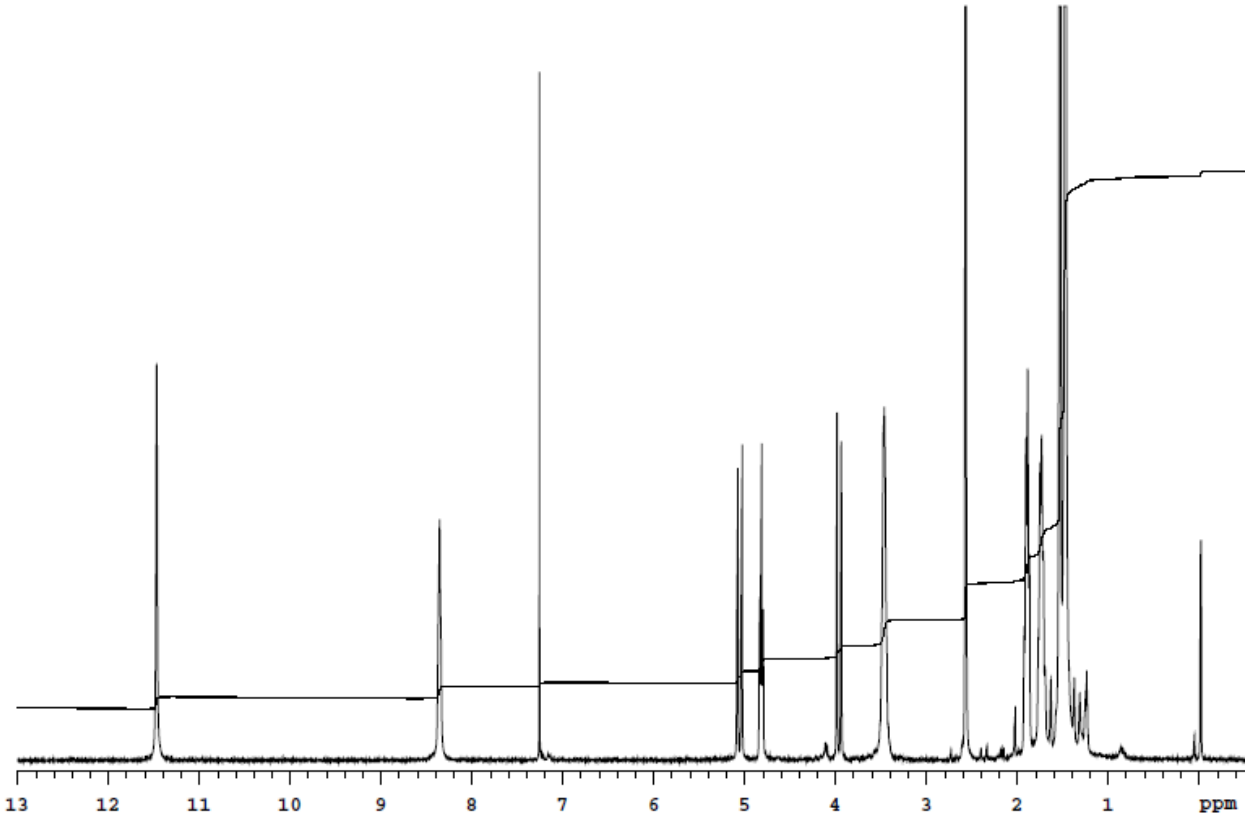
13
12
11
10
9
8
7
6
5
4
3
2
1
ppm

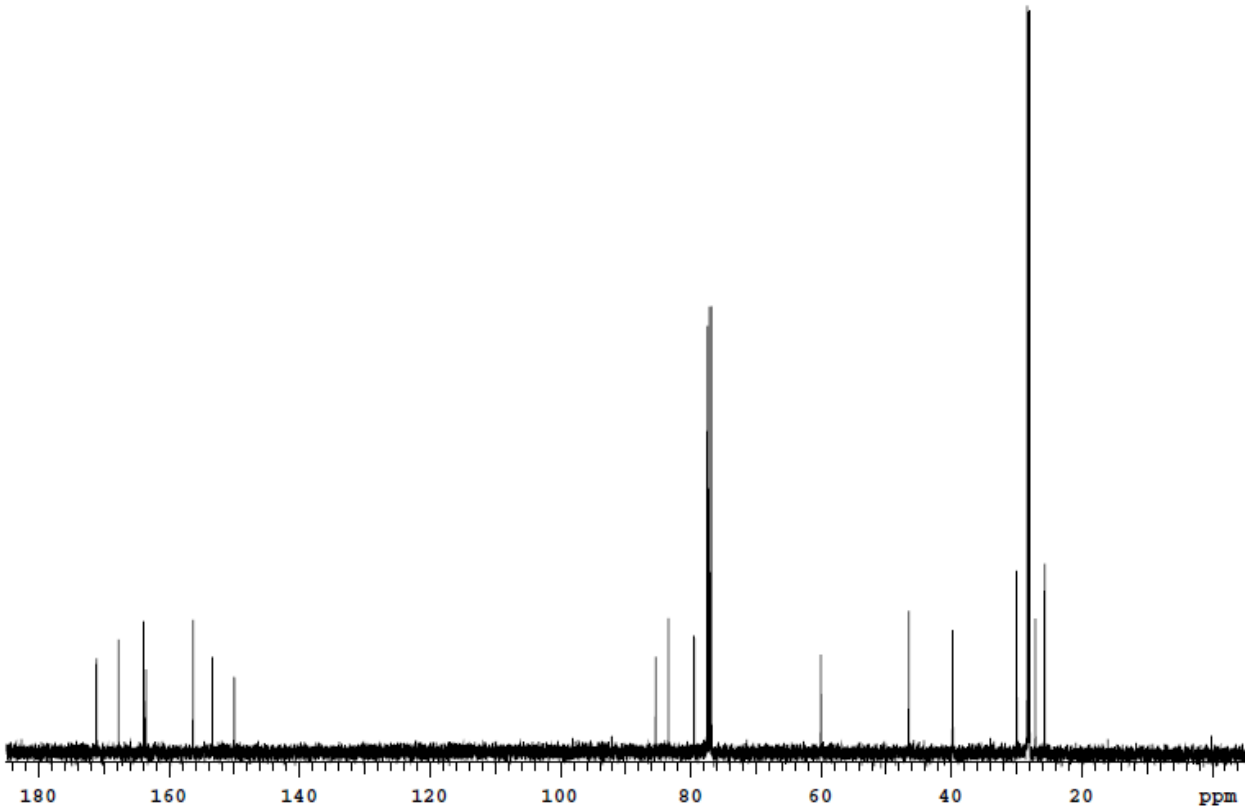
180
160
140
120
100
80
60
40
20
ppm

----- ----- ----- ----- ----- -----

13 in $CDCl_3$ (400 MHz).

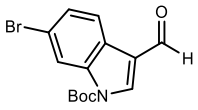

Full-size ^1H NMR:

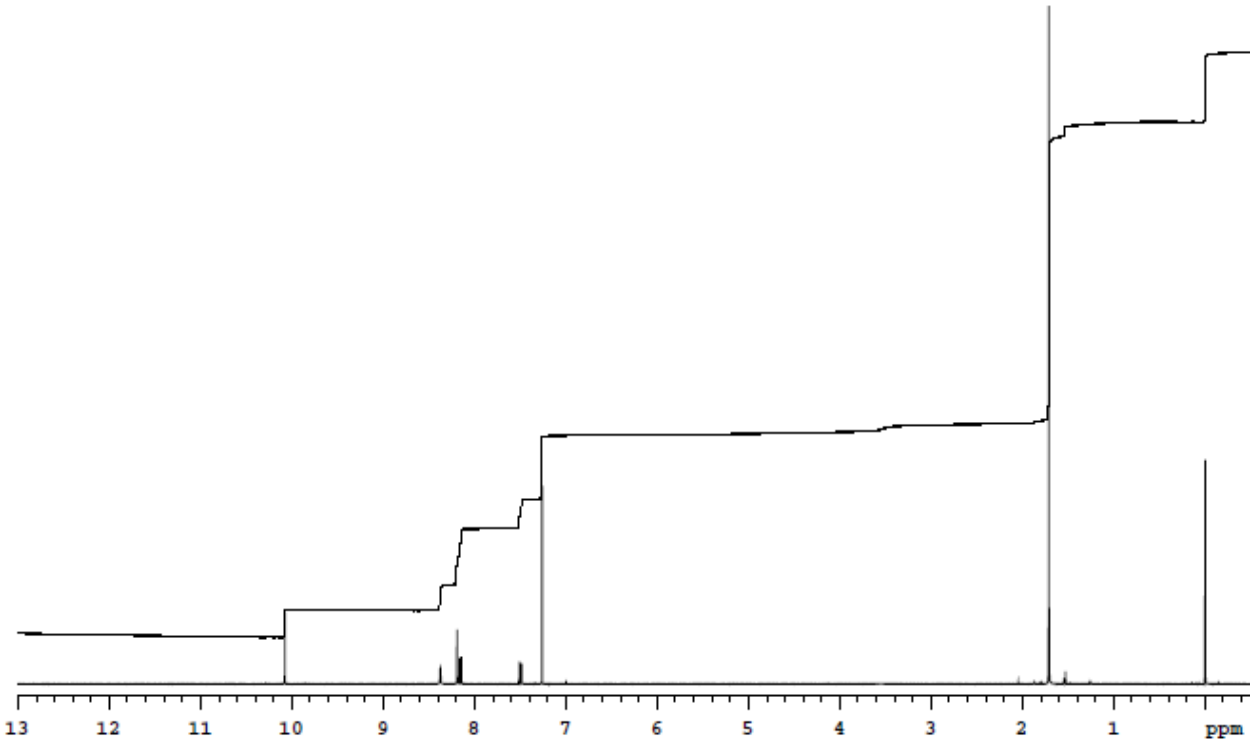

Vertically expanded ^1H peaks for clarity:

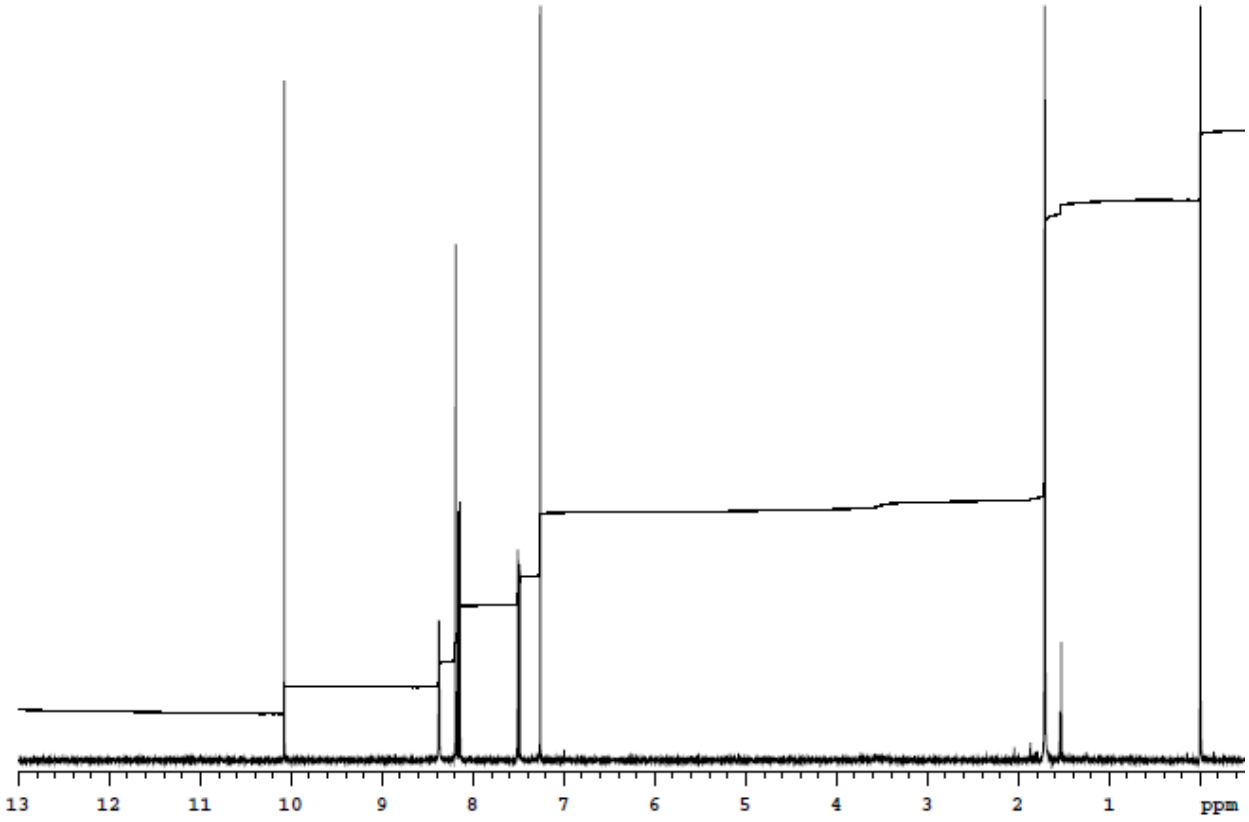

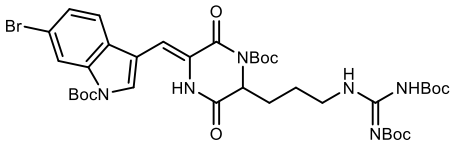

14 in $CDCl_3$ (400 MHz).

Full-size ^1H NMR:

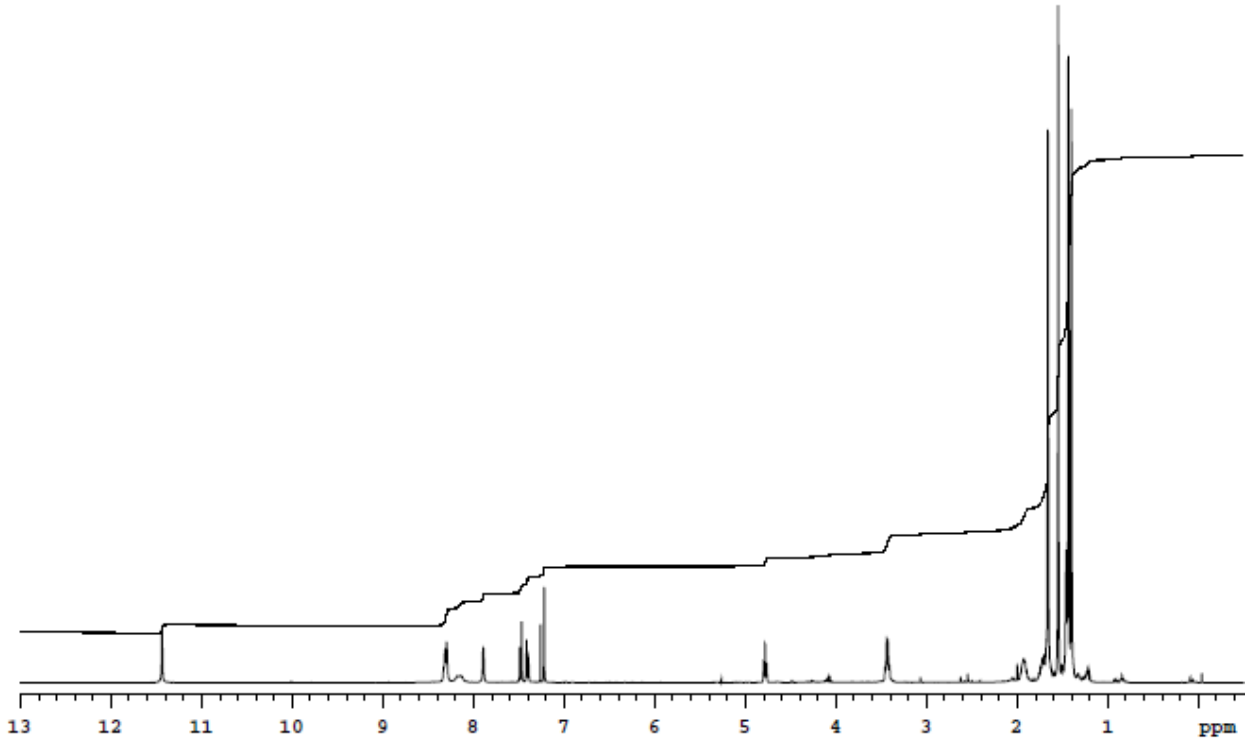

Vertically expanded ^{1}H peaks for clarity:

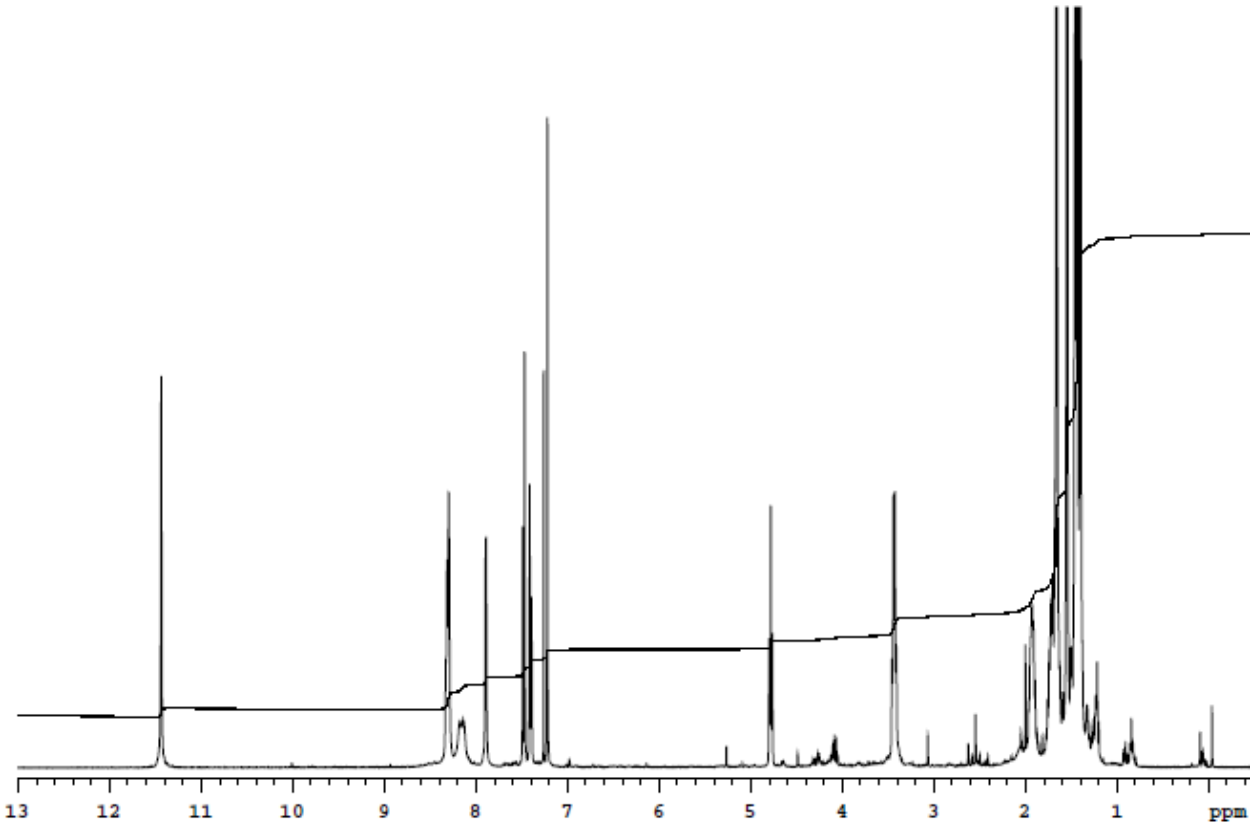

Full-size ^{13}C NMR:

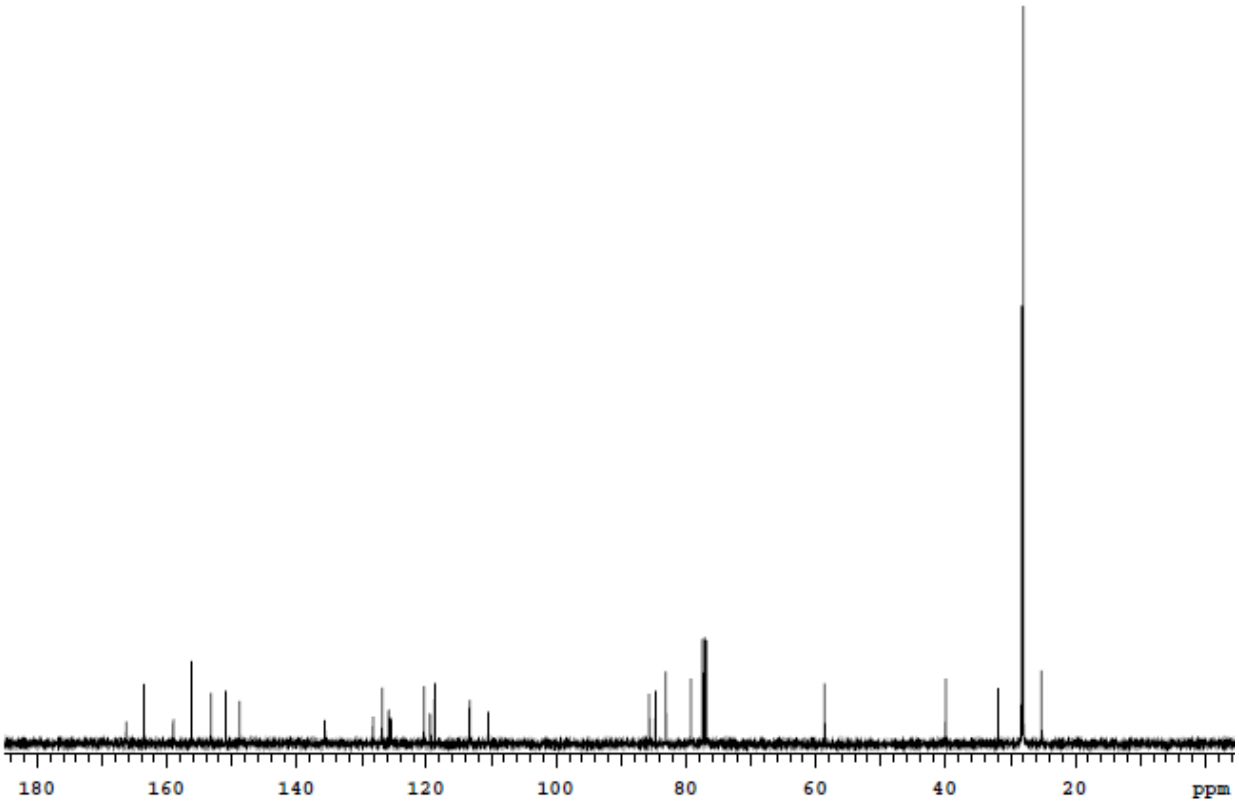

Vertically expanded ^{13}C peaks for clarity:

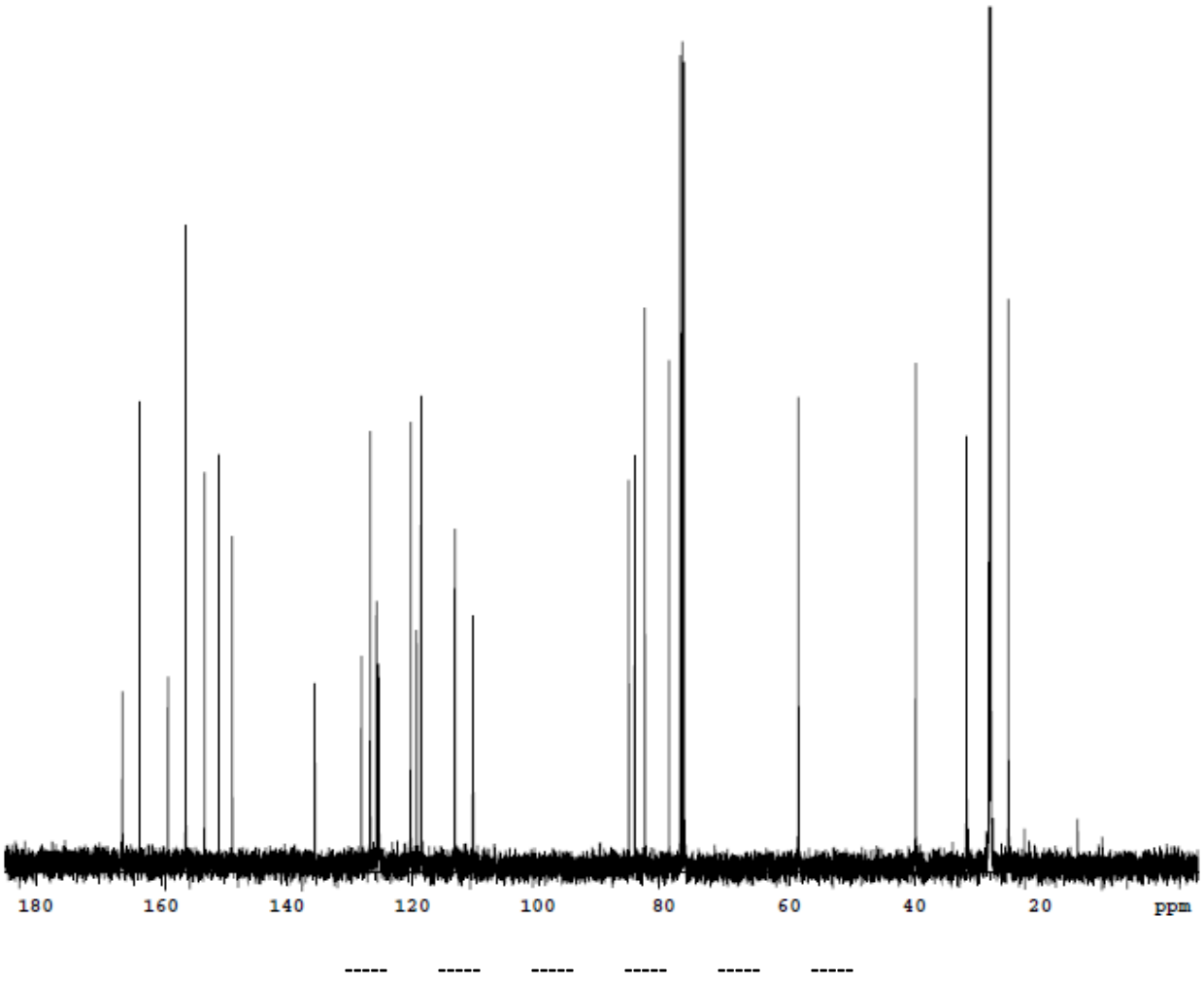

(±)-1• HO_2CCF_3 in DMSO-d_6 (400 MHz).

Full-size ^{1}H NMR:

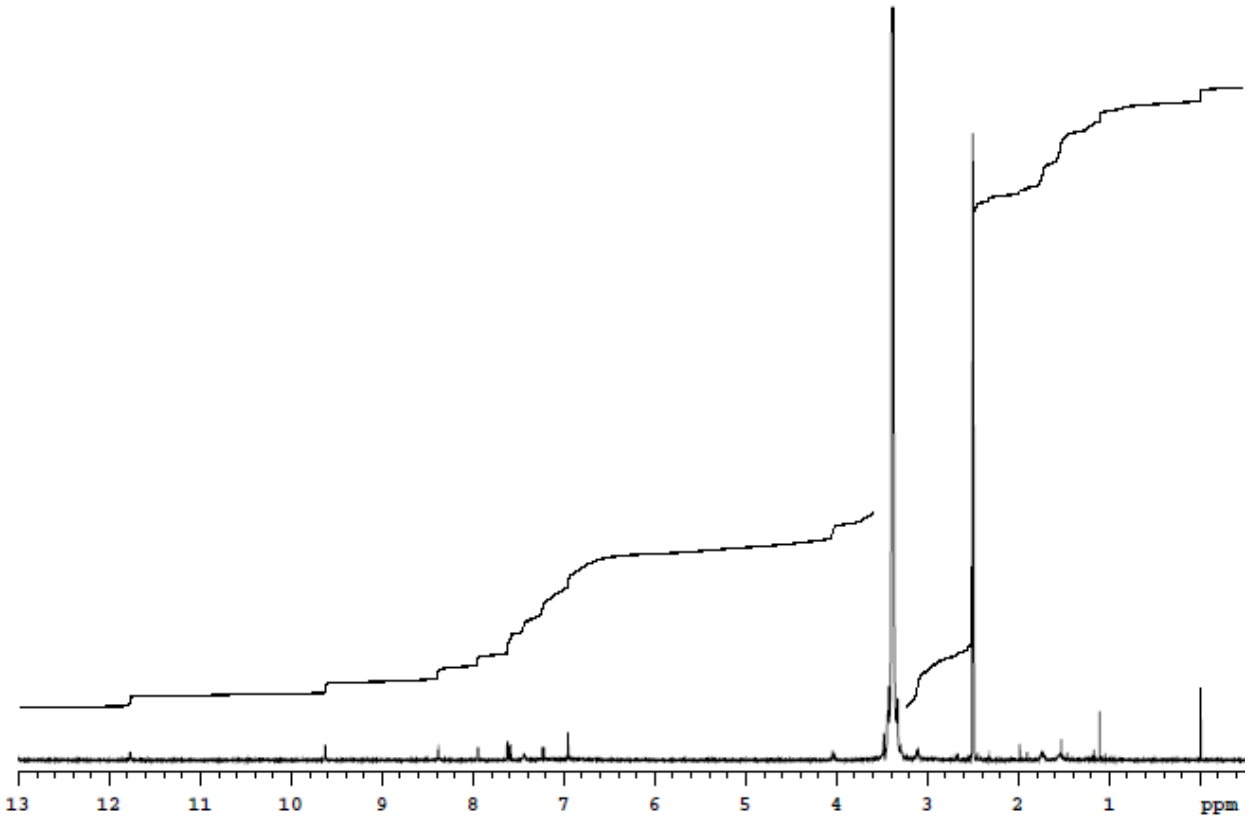

Vertically expanded ^{1}H peaks for clarity:

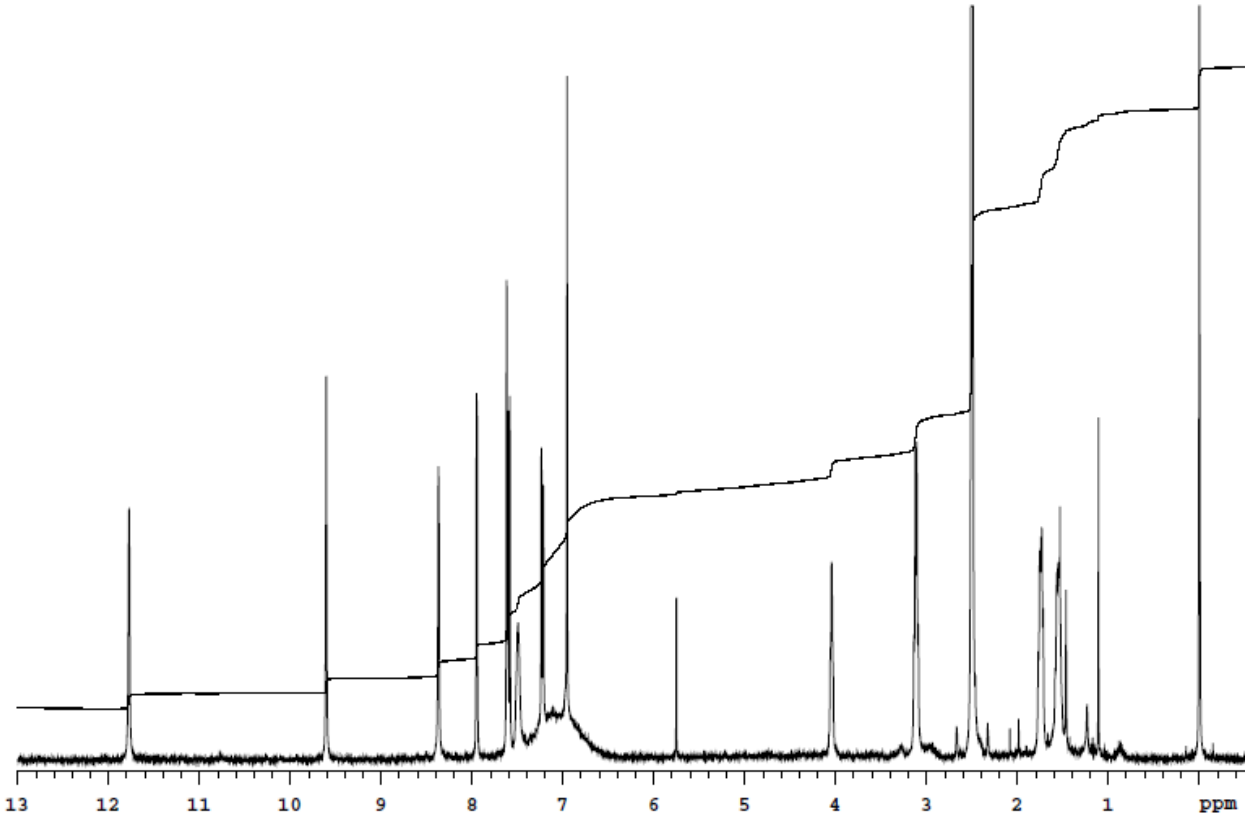

Full-size ^{13}C NMR: